bioRxiv preprint doi: https://doi.org/10.1101/495085; this version posted December 24, 2018. The copyright holder for this preprint (which was not certified by peer review) is the author/funder, who has granted bioRxiv a license to display the preprint in perpetuity. It is made available under a CC-BY 4.0 International license.

Nitric oxide radicals are emitted by wasp eggs to kill mold fungi

Short title: wasp eggs emit nitric oxide

Authors:

Erhard Strohm[a1], Gudrun Herzner[a], Joachim Ruther[b], Martin Kaltenpoth[a,c,d], Tobias Engl[a,c,d]

Affiliations:

[a] Evolutionary Ecology Group, Institute of Zoology, University of Regensburg, 93053 Regensburg, Germany.

[b] Chemical Ecology Group, Institute of Zoology, University of Regensburg, 93053 Regensburg, Germany.

[c] Insect Symbiosis Research Group, Max Planck Institute for Chemical Ecology, Hans-Knoell-Str. 8, 07745 Jena, Germany.

[d] current address: Evolutionary Ecology, Institute of Organismic and Molecular Evolution, Johannes Gutenberg University, Johann-Joachim-Becher-Weg 13, 55128 Mainz, Germany.

[1]To whom correspondence may be addressed. Erhard Strohm: Evolutionary Ecology Group, Institute of Zoology, University of Regensburg, 93053 Regensburg, Germany.

Email: erhard.strohm@ur.de, Tel. +49 941 9433072.

bioRxiv preprint doi: https://doi.org/10.1101/495085; this version posted December 24, 2018. The copyright holder for this preprint (which was not certified by peer review) is the author/funder, who has granted bioRxiv a license to display the preprint in perpetuity. It is made available under a CC-BY 4.0 International license.

Abstract: Detrimental microbes caused the evolution of a great diversity of antimicrobial defenses in plants and animals. Here we show that the eggs of a solitary digger wasp, the European beewolf *Philanthus triangulum,* emit large amounts of the gaseous free radical nitric oxide ($NO^{\cdot}$) to protect themselves and their provisions, paralyzed honeybees, against mold fungi. Despite the extraordinary concentrations of nitrogen radicals ($NO^{\cdot}$ and its oxidation product $NO_2^{\cdot}$) in the brood cells (~1500ppm), $NO^{\cdot}$ is synthesized from L-arginine by an NO-synthase (NOS) as in other animals. The beewolf *NOS* gene revealed no conspicuous differences to related species. However, due to alternative splicing, the NOS-mRNA in beewolf eggs lacks a 144bp exon near the regulatory domain. This preventive external application of high doses of $NO^{\cdot}$ by seemingly defenseless wasp eggs represents an evolutionary key innovation that adds a remarkable novel facet to the array of functions of the important biological effector $NO^{\cdot}$.

Introduction

Microbes pose a major threat to the health of all animals and plants. These have responded by evolving a great diversity of defenses including hygienic behaviors [1], antimicrobial chemicals [2-4], complex immune systems [5,6], and defensive symbioses [7,8]. Besides such pathogenic effects, many bacteria and fungi are severe, but often neglected, competitors of animals for nutrients, thus prompting the evolution of mechanisms to preserve food sources [9,10].

Some animals are particularly prone to suffer from microbial attack due to (1) high abundance of potentially harmful microbes in their environment, (2) a microbe-friendly microclimate and/or (3) limited defense mechanisms. The progeny of many insect species develop under warm and humid conditions in the soil, where they are exposed to a high diversity of bacteria and fungi. Moreover, compared to adult insects, immature stages, in particular eggs, have usually reduced abilities to prevent microbial infestation due to, for example, a thin cuticle or an inability to groom [11,12]. The situation is even aggravated when eggs and larvae have to develop on limited amounts of provisions that are susceptible to attack by ubiquitous and fast growing putrefactive bacteria and mold fungi [9,13].

Such hostile conditions prevail in nests of subsocial Hymenoptera like the European beewolf *Philanthus triangulum* (Hymenoptera, Crabronidae). The offspring of these solitary digger wasps develop in subterranean brood cells provisioned by the female wasps with paralyzed honeybee workers (*Apis mellifera*, Apidae, Hymenoptera) [14] (Fig. 1A). The beewolf egg is laid on one of the bees, the larva hatches after three days, feeds on the bees for six to eight days, then spins a cocoon and either emerges the same summer or hibernates. The warm and humid microclimate in the brood cell promotes larval development, but also favors fast growing, highly detrimental fungi

[15]. Without any countermeasures the provisions will be completely overgrown by mold fungi within three days (Fig. 1B), and the beewolf larva becomes infested by fungi or starves to death [16,17].

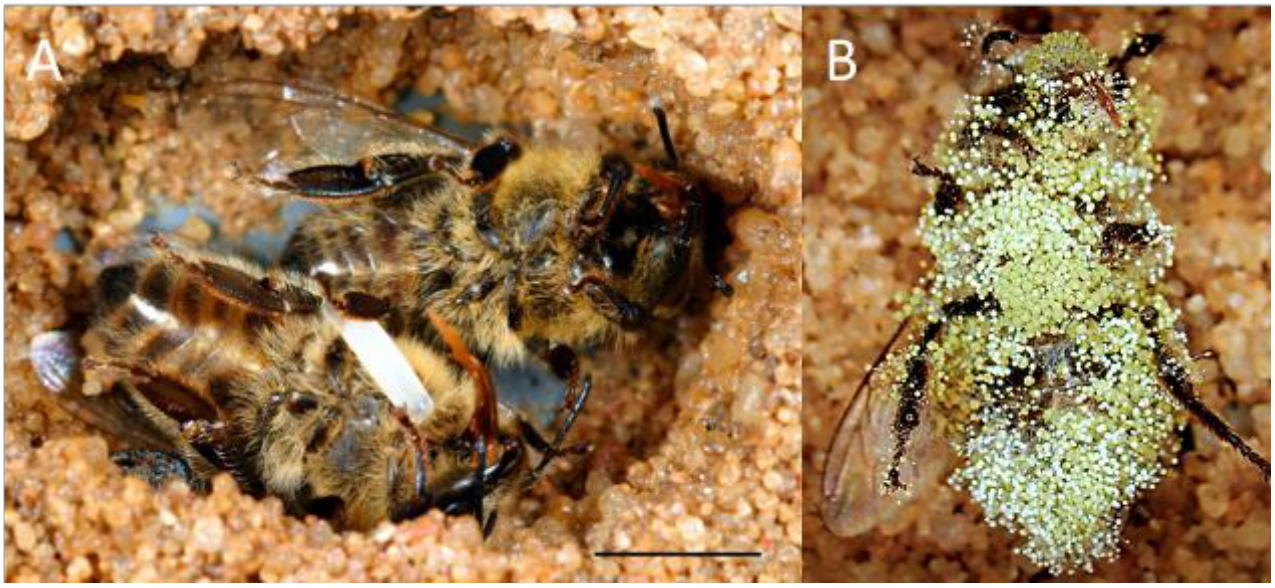

Figure 1. (A) Brood cell of the European beewolf with two bees, one carrying an egg, in an observation cage. (B) Honeybee paralyzed by a beewolf female but immediately removed and kept in an artificial brood cell, heavily overgrown by mold fungi that have already developed conidia. Scale bar = 5mm.

We have previously documented how beewolf females reduce molding of the larval provisions by coating the paralyzed bees with ample amounts of unsaturated hydrocarbons [18]. This embalming changes the physicochemical properties of the preys' surface causing reduced water condensation on the bees [19]. Due to the deprivation of water, germination and growth of fungi is delayed by two to three days [20]. Despite this considerable effect, when removed from brood cells at least 50% of embalmed bees showed fungus infestation within six days after oviposition [16]. Since in natural brood cells only around 5% of the progeny succumb to mold fungi [16], we searched for an additional antimicrobial defense mechanism.

78 Here we report on a unique antifungal strategy that is employed by beewolf eggs to defend
79 themselves and their provisions against mold fungi. Employing bioassays we discovered that
80 beewolf eggs emit a strong antifungal agent that we identified as the gaseous radical nitric oxide
81 ($NO^{\cdot}$). We characterize the amount and time course of emission and, using histological methods,
82 inhibition assays, and gene expression analysis, we elucidate the biosynthetic pathway of $NO^{\cdot}$ in
83 beewolf eggs. To explore the evolutionary background of this remarkable antimicrobial strategy,
84 we sequenced the relevant gene and mRNA. Our findings reveal a novel function of the eminent
85 biological effector $NO^{\cdot}$ in providing an extended immune defense to the producer by sanitizing its
86 developmental microenvironment.
87
88

bioRxiv preprint doi: https://doi.org/10.1101/495085; this version posted December 24, 2018. The copyright holder for this preprint (which was not certified by peer review) is the author/funder, who has granted bioRxiv a license to display the preprint in perpetuity. It is made available under a CC-BY 4.0 International license.

Results

Emission of an antifungal volatile by beewolf eggs

Thorough examination of beewolf nests in observation cages [21] revealed that within 24 h after oviposition, a conspicuous pungent smell emanated from the eggs. We hypothesized that this smell was due to an antifungal agent. When paralyzed honeybees from completed beewolf brood cells were incubated individually, bees carrying an egg showed significantly delayed fungus growth compared to bees without egg over the period from oviposition to cocoon spinning (Kaplan Meier survival analysis, Breslow test, day 0-11: Chi square = 12, df = 1, p = 0.001; Fig. 2A). This difference was also significant for the period from oviposition to the hatching of the larvae (day 0-3: Chi square = 9.5, df = 1, p = 0.002), suggesting that this effect is not due to possible antifungal mechanisms of the larvae but that it is mediated by the egg. Considering the distinctive odor that emanated from the eggs, we tested whether the antifungal effect is caused by a volatile agent. Two experiments supported this assumption. First, provisioned bees without wasp eggs that were kept in artificial brood cells together with bees carrying an egg (but without physical contact) showed significantly delayed fungal growth compared to control bees that were kept alone (Breslow test, day 0-11: Chi square = 7.6 df = 1, p = 0.006; day 0-3: Chi square = 9.1, df = 1, p = 0.003; Fig. 2B). Second, when one of the most abundant mold species from infested beewolf brood cells, the fast growing *Aspergillus flavus* [15], was exposed to the volatiles presumably emanating from beewolf eggs on nutrient agar for three days, its growth was entirely inhibited, whereas it thrived in controls (binomial test: N = 20, $p < 0.001$, Fig. 3). In analogous bioassays, five other fungal strains (*A. flavus* strain B*, Mucor circinelloides, Penicillium roqueforti, Candida albicans* and *Trichophyton rubrum*) were similarly inhibited when exposed to volatiles from beewolf eggs (for each strain N = 8, $p < 0.01$). Notably, when the beewolf larvae were removed from the assays shortly after hatching (three days after oviposition), no fungal growth occurred in

113 the exposed areas during another three days. We conclude that beewolf eggs release a volatile
114 compound with broad spectrum fungicidal properties.
115

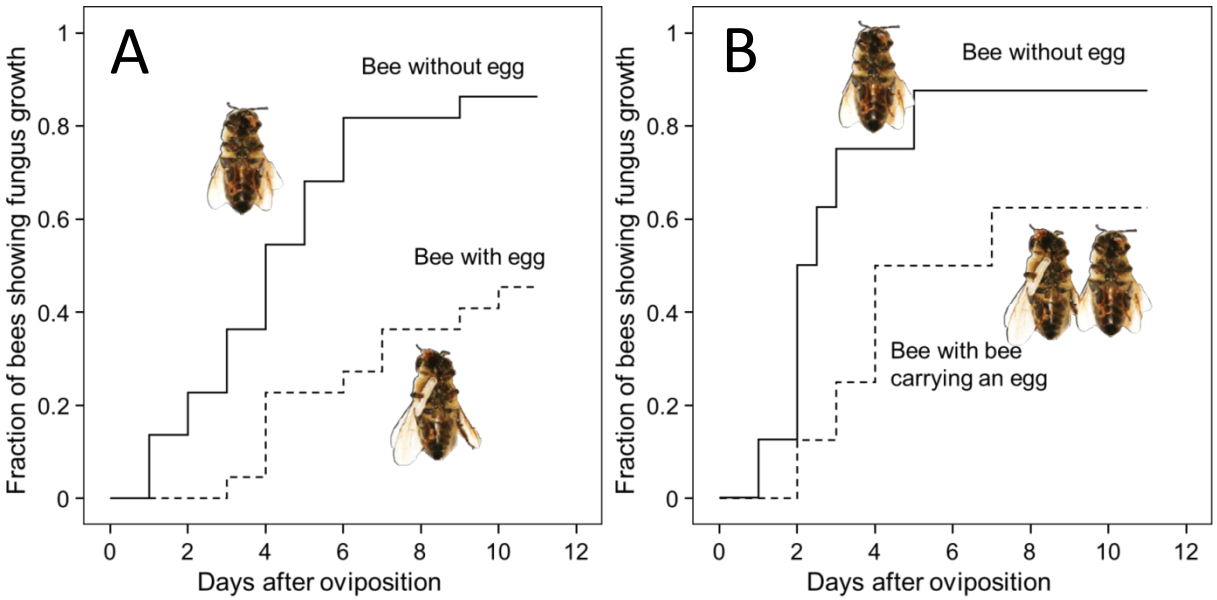

116

117 **Figure 2**. Onset of fungal growth on paralyzed honeybees taken from *Philanthus triangulum* nests and kept
118 in artificial brood cells. The fraction of bees showing first signs of fungal growth is shown as a function of
119 days since oviposition. (A) Honeybees that either carried an egg (dashed line) or not (solid line) (N = 22
120 each, hazard ratio = 0.43). (B) Honeybees that were either kept alone (solid line) or shared a brood cell with
121 a bee carrying an egg (dashed line) (N = 16 each, hazard ratio = 0.49). Source data file: Fig 2 Source data –
122 effect of egg on fungus growth.xlsx
123
124

bioRxiv preprint doi: https://doi.org/10.1101/495085; this version posted December 24, 2018. The copyright holder for this preprint (which was not certified by peer review) is the author/funder, who has granted bioRxiv a license to display the preprint in perpetuity. It is made available under a CC-BY 4.0 International license.

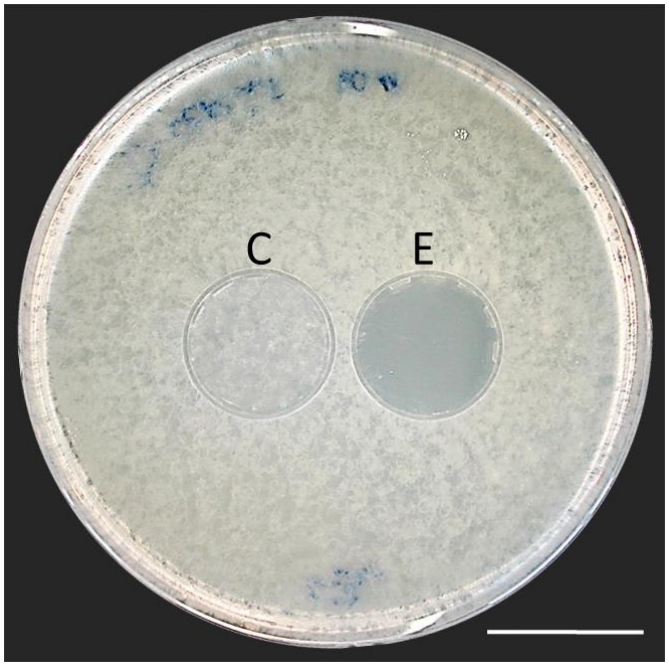

Figure 3. Bioassay demonstrating the inhibitory effect of a beewolf egg against *Aspergillus flavus*. Two areas on the agar were covered by caps of a volume similar to natural beewolf brood cells. One cap, the control (C), was empty, while the experimental cap (E) contained a fresh beewolf egg attached to the ceiling of the cap. The caps were removed and the picture was taken after 24 h of incubation at 25°C. The control area (C) shows dense whitish fungal hyphae similar to the surroundings. However, the area that was exposed to the volatiles from a beewolf egg (E) shows bare agar, indicating that the growth of this aggressive fungus was entirely inhibited. Scale bar = 2.5 cm

Identification of the antifungal volatile

The odor emanating from the eggs was similar to that of highly reactive oxidants such as chlorine, ozone and nitrogen dioxide [22]. The most likely candidate was the radical nitrogen dioxide ($NO_2^{\cdot}$), because there is a plausible way for it to be generated by wasp eggs: Insect embryos synthesize small amounts of nitric oxide ($NO^{\cdot}$) as signaling effectors for developmental processes [23]. If such odorless $NO^{\cdot}$ was emitted from the egg, it would spontaneously react with oxygen [24,25] to yield the strong-smelling $NO_2^{\cdot}$. Moreover, belonging to the reactive nitrogen species (RNS), $NO^{\cdot}$ and $NO_2^{\cdot}$ show considerable antimycotic activity [26,27] that would explain the observed fungicidal effect of beewolf eggs.

bioRxiv preprint doi: https://doi.org/10.1101/495085; this version posted December 24, 2018. The copyright holder for this preprint (which was not certified by peer review) is the author/funder, who has granted bioRxiv a license to display the preprint in perpetuity. It is made available under a CC-BY 4.0 International license.

143

144 We conducted a series of experiments to determine whether beewolf eggs produce and emit $NO^{\cdot}$
145 and/or $NO_2^{\cdot}$. First, headspace samples of confined beewolf eggs were subjected to the Griess
146 assay, the standard procedure for the specific detection of $NO^{\cdot}$ and $NO_2^{\cdot}$ [28]. The emerging red
147 color of the resulting azo dye clearly indicated the presence of $NO^{\cdot}/NO_2^{\cdot}$. To visualize the emission
148 of $NO^{\cdot}$ from beewolf eggs, we sprayed a solution of an $NO^{\cdot}$ specific fluorescent probe,
149 Diaminorhodamin-4M AM (DAR4M-AM), onto prey bees carrying freshly laid eggs. The small
150 droplets of the DAR4M-AM solution on the bees showed a clear fluorescence around the egg that
151 increased over several hours (Fig. S1B). No such effect was seen on control bees without eggs (Fig.
152 S1A). Moreover, beewolf eggs injected with the DAR4M-AM solution showed a strong
153 fluorescence that peaked about one day after oviposition (N = 45, Fig. 4A). The same treatment
154 yielded only weak fluorescence in the eggs of two other Hymenoptera (the Emerald cockroach
155 wasp, *Ampulex compressa*, N = 9, and the Red mason bee, *Osmia bicornis*, N = 12; Figs. 4C and D)
156 and in newly hatched beewolf larvae (N = 4, not shown). Autofluorescence of beewolf eggs
157 injected with buffer only (N = 10) was negligible (Fig. 4B). These findings strongly imply that
158 beewolf eggs produce and release $NO^{\cdot}$, which spontaneously reacts with oxygen to $NO_2^{\cdot}$ radicals.

159

160 **Figure S1**. Visualization of $NO^{\cdot}$ emission by beewolf eggs using fluorescence imaging. (A) Honeybee from a
161 brood cell without an egg and (B) honeybee with egg. Both bees were sprayed with a solution of the $NO^{\cdot}$
162 specific fluorescence probe DAR4M-AM. Only the droplets on the bee with the egg (B) show a bright yellow
163 and orange fluorescence indicating the presence of $NO^{\cdot}$. Image is a composite of multiple pictures of the x/y
164 plane and z-axis. Scale bar = 1 mm.

165

166 Amount and time course of $NO^{\cdot}$ emission

Using iodometry, we determined that a beewolf egg emits on average 0.25 ± 0.09 µmol $NO^{\cdot}$ (N = 233). The rate of $NO^{\cdot}$ production was initially very low, but increased to a distinct peak 14-15 h (at 28°C) after oviposition (Fig. 5); around 90 % of $NO^{\cdot}$ emission occurred within a two-hour period. Assuming no loss due to reactions or leaking out of the confined space of brood cells (volume 3.2 ± 0.9 cm^3, N = 250), the nitrogen oxides would accumulate to average concentrations of 1690 ± 680 ppm. The timing of the onset of $NO^{\cdot}$ emission was strongly temperature dependent (Fig. S2), with higher temperatures resulting in an earlier $NO^{\cdot}$ production (temperature coefficient Q_{10} = 2.74).

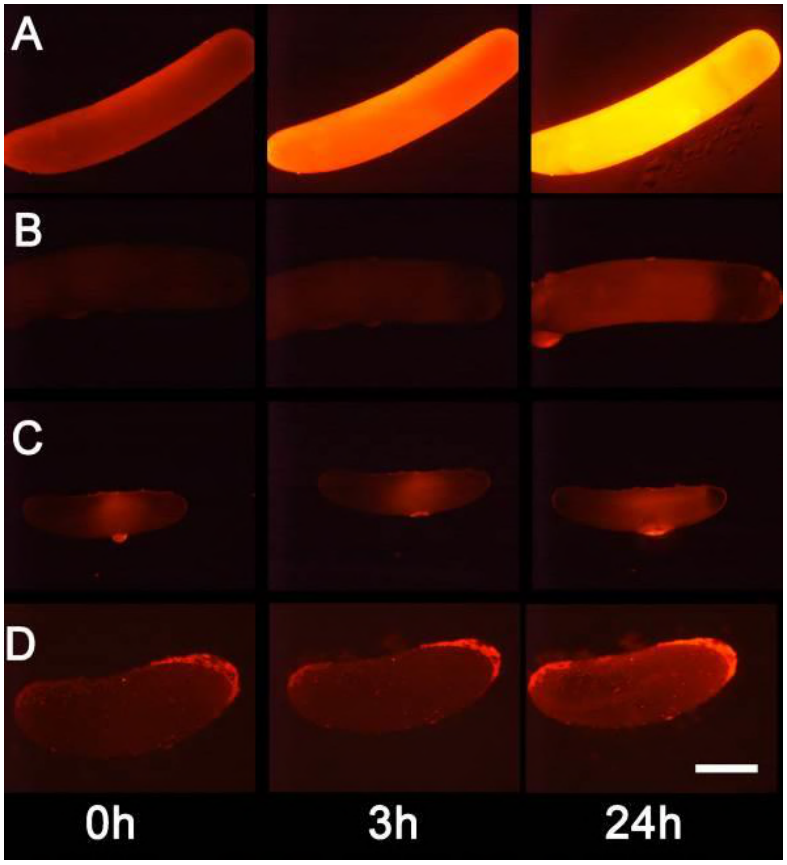

Figure 4. Detection of nitric oxide ($NO^{\cdot}$) in beewolf eggs. Newly laid eggs of beewolves, *Philanthus triangulum*, of the cockroach wasp *Ampulex compressa* and of the Red Mason bee, *Osmia bicornis* were injected with the $NO^{\cdot}$ sensitive fluorescence probe DAR4M-AM. Control beewolf eggs were injected with phosphate buffer. Images were obtained by fluorescence microscopy 0, 3 and 24 h after injection. Row A: DAR4M-AM injected beewolf egg showing strong increase in fluorescence; B: Buffer-injected control

beewolf egg showing the level of autofluorescence; C: DAR4M-AM injected egg of *A. compressa;* D: DAR4M-AM injected egg of *O. bicornis*. Scale bar: 1 mm.

Figure S2. Start of $NO^{\cdot}$ emission (h after oviposition) as a function of temperature. Beewolf eggs were kept at different temperatures and the onset of $NO^{\cdot}$ release was assessed using the color change of an iodide starch solution as monitored by a digital camera at 30min intervals. Symbols are means ± SD (Quadratic regression: $R^2 = 0.98$, N = 33, $p < 0.001$; $Q_{10} = 2.74$). Source data file: Fig S2 Source data - start of NO emission.xlsx

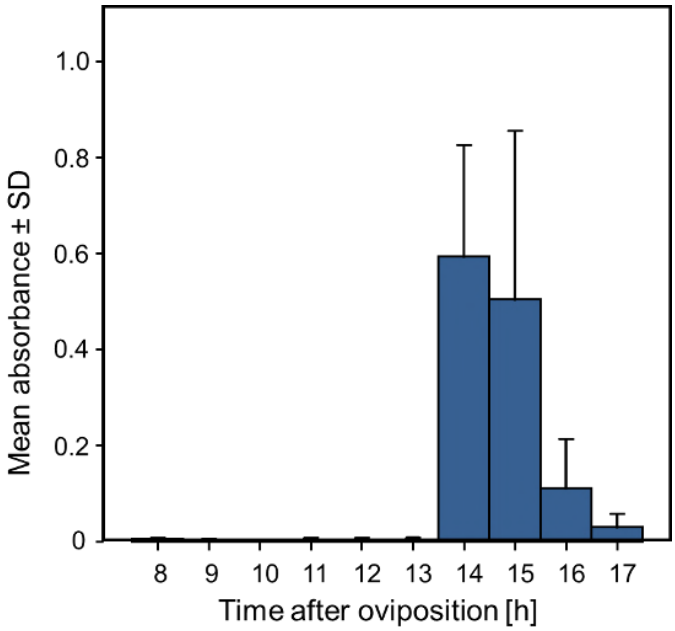

Figure 5. Timing of $NO^{\cdot}$ emission from beewolf eggs (N = 4). The photometrically determined absorbance at 590 nm (mean ± SD) is shown as a function of time after oviposition for iodide-starch solutions successively exposed to beewolf eggs for one hour. Source data file: Fig 5 Source data - timing of NO emission.xlsx

Synthesis of $NO^{\cdot}$ in beewolf eggs

Eukaryotes synthesize $NO^{\cdot}$ from the amino acid L-arginine by the enzyme nitric oxide synthase (NOS) [29] which is highly conserved also in insects [30]. The exceptional level of $NO^{\cdot}$ emission of

bioRxiv preprint doi: https://doi.org/10.1101/495085; this version posted December 24, 2018. The copyright holder for this preprint (which was not certified by peer review) is the author/funder, who has granted bioRxiv a license to display the preprint in perpetuity. It is made available under a CC-BY 4.0 International license.

beewolf eggs raised the question of whether they employ the same pathway or have evolved a different mechanism. Using the fixation insensitive nicotinamide-adenine-dinucleotide phosphate (NADPH) -diaphorase assay, we found evidence for NOS activity of embryonic tissue in beewolf eggs (Fig. S3). Moreover, by employing reverse transcription and real time quantitative PCR, we revealed that the temporal expression pattern of NOS-mRNA showed a clear peak around the time of maximum $NO^{\cdot}$ emission (Fig. S4). To directly test for the involvement of NOS we injected beewolf eggs with Nω-nitro-L-arginine methylester (L-NAME), a NOS-inhibiting analogue of L-arginine. This treatment caused a significant decrease in $NO^{\cdot}$ emission, whereas the non-inhibiting enantiomer D-NAME had no such effect (Fig.6). We therefore conclude that in beewolf eggs, $NO^{\cdot}$ is synthesized from L-arginine via NOS.

Figure S3. Photomicrograph of a longitudinal section of a beewolf egg showing fixation insensitive NADPH-diaphorase activity. Strong blue staining in the embryonic tissue indicates the presence of reduced nitroblue tetrazolium demonstrating NOS activity (c=cuticle, s=serosa, e= embryo, a=amnion, ac= amnion cavity, scale bar = 1 mm, image composed from two separate photos of the left and right parts of the egg.).

Figure S4. Gene expression of NOS relative to ß-actin in beewolf eggs at different times after oviposition and in freshly hatched larvae. Two trials were conducted, one with 19 and one with 24 eggs per time point. Mean ratios of NOS-mRNA to ß-Actin-mRNA are shown (with standard deviations), as determined by Q-RT-PCR. Source data file: Fig S4 Source data - NOS gene expression.xlsx

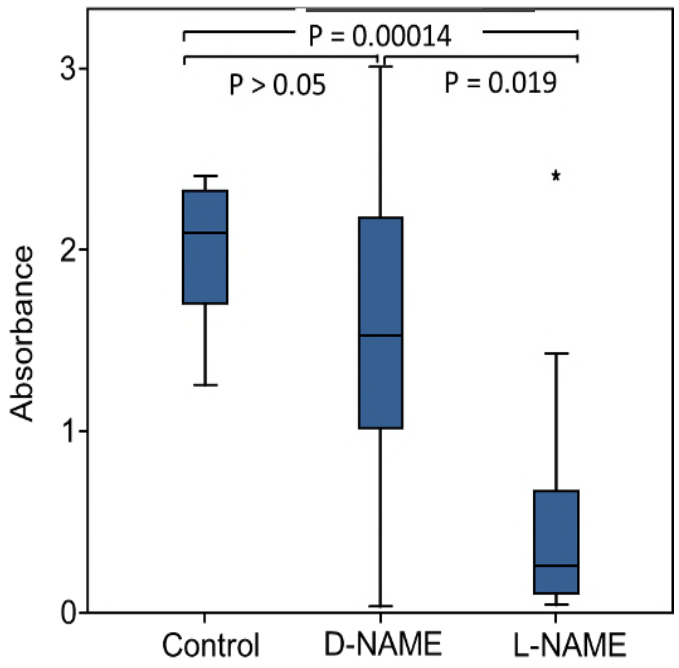

Figure 6. Effect of NOS inhibition on $NO^{\cdot}$ production. Amount of $NO^{\cdot}$ and/or $NO_2^{\cdot}$ emanating from non-injected beewolf eggs (control) and those injected with D-NAME (a non-inhibiting enantiomer of L-NAME) or L-NAME (a NOS inhibiting L-arginine analogue). The photometrically determined absorbance at 590 nm is shown for iodide-starch solutions that were exposed for 24 h to the headspace of eggs of the indicated treatment group (shown are median, quartiles and range, * indicates an outlier, included in the analysis). P-values are for Holm-corrected Mann-Whitney U-tests. Source data file: Fig 6 source data – NOS inhibition.xlsx

The beewolf *NOS*-gene and NOS-mRNA in eggs

In contrast to vertebrates, most invertebrates appear to have only one type of NOS [31,32]. Considering the high level of $NO^{\cdot}$ production in beewolf eggs, we hypothesized that beewolves have more than one *NOS* gene or that the NOS responsible for the $NO^{\cdot}$ synthesis in beewolf eggs might exhibit considerable changes in enzyme structure compared to the NOS of related species. Sequencing of the *NOS*-gene(s) of *P. triangulum* (*Pt-NOS*) revealed only one *Pt-NOS* copy in the beewolf genome comprising 9.36 kbp with 25 exons (Fig. S5). A phylogenetic analysis of the

bioRxiv preprint doi: https://doi.org/10.1101/495085; this version posted December 24, 2018. The copyright holder for this preprint (which was not certified by peer review) is the author/funder, who has granted bioRxiv a license to display the preprint in perpetuity. It is made available under a CC-BY 4.0 International license.

246 resulting amino acid sequence revealed a high similarity to the NOS of the closely related bees
247 (Apidae, Fig. S6). However, mRNA sequencing showed that, in contrast to adult beewolves and
248 honeybees, the NOS-mRNA of beewolf eggs (3.72 kbp) lacks exon 14 comprising 144 bp. In the
249 NOS-mRNA of adult beewolves this exon is located between the binding domains for calmodulin
250 and flavin mononucleotide (FMN) (Fig. S5).

251

252 **Figure S5**. Structure of the *Pt-NOS* gene indicating position and length of exons. Exon 14 (red) is missing in
253 the NOS mRNA in beewolf eggs compared to adults. Presumed cofactor-binding domains as deduced from
254 homologous sequences of the *NOS* of *Anopheles stephensi* [68, 69] are indicated for heme, calmodulin
255 (CaM), FMN, FAD pyrophosphate (FAD PPi) and FAD isoalloxazine (FAD Iso), NADPH ribose, NADPH adenine,
256 and NADPH.

257

258 **Figure S6**. Consensus tree obtained from Bayesian analysis of NOS amino acid sequences from five orders
259 of insects (distinguished by different colors), including the NOS sequences of *P. triangulum* eggs (lowermost
260 entry). Values at the nodes represent Bayesian posterior probabilities and local support values (FastTree
261 analysis), respectively. Scale bar represents 0.1 changes per site.

262

263

264

bioRxiv preprint doi: https://doi.org/10.1101/495085; this version posted December 24, 2018. The copyright holder for this preprint (which was not certified by peer review) is the author/funder, who has granted bioRxiv a license to display the preprint in perpetuity. It is made available under a CC-BY 4.0 International license.

Discussion

Fighting pathogens is of outstanding importance for any organism and has driven the evolution of a great diversity of antimicrobial defenses. Internal immune systems have been extensively documented especially in vertebrates [33-34] but also in insects [35,36], including insect eggs [37]. However, comparatively little is known about external antimicrobial strategies that provide protection for the own body, for the progeny, or for food. There are some reports on the application of antimicrobial secretions on the body surface by adult insects [11,38] or inside a host by larvae of a parasitoid wasp [2]. Carrion beetles preserve the larval food, buried carcasses, by application of antimicrobials [39]. Females of some insect species deposit antimicrobial chemicals [40,41] or antibiotics producing symbiotic bacteria [8, 42] onto their eggs and ant workers can counter microbial infestation of the brood by applying venom [43]. Recently, the employment of volatile antimicrobials by insects as a means of external defense has gathered some interest [4,44.45].

Like other insects that develop in the soil, beewolves are particularly menaced by a diverse and unpredictable range of detrimental microbes. In fact, beewolf progeny and their provisions are under severe threat from fast growing mold fungi [16]. As a consequence, beewolves have evolved at least three very different antimicrobial defenses that provide an effective, coordinated, and enduring protection against a broad spectrum of microbes during the whole development. First, throughout the long period of winter diapause prior to emergence progeny are protected by antibiotics on their cocoons that are produced by symbiotic *Streptomyces* bacteria [7,46,47]. Second, during the early egg and larval stages, molding of the provisions is retarded by an embalming of the honeybees with lipids by the mother wasp [16]. Third, as shown here, the emission of gaseous nitrogen oxide radicals by the beewolf egg might be the most important of

bioRxiv preprint doi: https://doi.org/10.1101/495085; this version posted December 24, 2018. The copyright holder for this preprint (which was not certified by peer review) is the author/funder, who has granted bioRxiv a license to display the preprint in perpetuity. It is made available under a CC-BY 4.0 International license.

289 the three antimicrobial mechanisms since it takes effect in a very early developmental phase and it
290 results not only in delay of molding but in killing of detrimental fungi in their immediate
291 environment. Thus brood cell fumigation provides beewolf offspring with a decisive initial
292 advantage over the fast growing mold fungi.
293
294 The emission of a gaseous agent by beewolf eggs to their confined brood cells is an ideal way to
295 sanitize such intricately structured surfaces as the bodies of honeybees and the rough walls of the
296 brood cell. $NO^{\cdot}$ seems to be a most suitable gaseous agent because it can obviously be produced
297 by beewolf eggs in amounts that effectively kill mold fungi in their brood cell. Such volatile
298 sanitation mechanisms that provide a front-line defense against microbes [4] will mostly be
299 inconspicuous and might turn out to be a wider theme in nature.
300
301 $NO^{\cdot}$ is an ancient biological effector of immense importance in all kinds of organisms ranging from
302 procaryotes to higher plants and animals [29, 48]. Owing to its high diffusibility across
303 biomembranes and specific chemical properties, this gaseous radical plays a crucial role in a
304 multitude of biological processes [29, 48]. In vertebrates, $NO^{\cdot}$ is synthesized from L-arginine by
305 three different isoforms of NOS that are encoded by different genes [29, 48]. Low levels of NO (<
306 1µmol/l) are produced by constitutive NOS (cNOS) isoforms (endothelial eNOS, neuronal nNOS)
307 and have signaling functions, e.g. in neuronal development and in the regulation of vascular tone
308 in vertebrates. Higher $NO^{\cdot}$ concentrations (1-10 µmol/l, [49]) are generated by an inducible NOS
309 (iNOS). At such levels $NO^{\cdot}$ is highly cytotoxic [49], making it a powerful antimicrobial [26,27], for
310 example in macrophages [29]. However, overproduction of $NO^{\cdot}$ due to inflammatory processes
311 [50] or certain diseases (e.g. Alzheimer's disease, [51]) may cause harmful side-effects [52] and
312 even septic shock [53]. Moreover, $NO^{\cdot}$ might affect carcinogenesis and tumor progression in a
313 positive as well as in a negative way [54].

bioRxiv preprint doi: https://doi.org/10.1101/495085; this version posted December 24, 2018. The copyright holder for this preprint (which was not certified by peer review) is the author/funder, who has granted bioRxiv a license to display the preprint in perpetuity. It is made available under a CC-BY 4.0 International license.

314

315 In living tissues, $NO^{\cdot}$ is usually removed within seconds by reacting with the heme group of
316 molecules such as oxyhemoglobin [55,56] (very low concentrations may still persist for hours [48]).
317 In air, the autooxidation to $NO_2^{\cdot}$ is comparatively slow so that $NO^{\cdot}$ persists (depending on its
318 concentration) for several seconds to minutes [25,56] or even hours [24]. Thus, the $NO^{\cdot}$ emitted by
319 beewolf eggs might directly affect fungi, e.g. by damaging DNA [27,57] or by reacting with the
320 heme group of enzymes like cytochrome P450 and cytochrome c oxidase, thus inhibiting these
321 crucial components of the mitochondrial respiratory chain [49,58,59,60]. Yet, most of the
322 antimicrobial activity of $NO^{\cdot}$ is attributed to indirect effects via reactive nitrogen species (RNS), in
323 particular nitrogen oxides ($NO_2^{\cdot}$, N_2O_3) and peroxynitrite ($ONOO^-$, upon reaction with superoxide)
324 [49]. $NO_2^{\cdot}$, has been reported to be severely cytotoxic, e.g. by nitration of tyrosine residues and
325 oxidation of proteins and lipids [26,60].

326

327 Even assuming some loss due to reactions or diffusion, the estimated maximum concentration of
328 nitrogen oxides ($NO^{\cdot}$ and $NO_2^{\cdot}$) in beewolf brood cells (more than 1500 ppm or 60 µmol/l) vastly
329 exceeds the concentrations in tissues (mostly lower than 0.1 µmol/l [56], 0.85-1.3µmol/l in muscle
330 tissue [61]). The maximum concentration in beewolf brood cells might thus be even higher than
331 what is used in medical applications against multiple drug resistant bacteria (200 ppm $NO^{\cdot}$ [62]) or
332 in antifungal treatment of fruit (50-500 ppm $NO^{\cdot}$ [63]) and is far beyond permissible exposure
333 limits for humans (e.g. for the USA: 25 ppm for $NO^{\cdot}$, 5 ppm for $NO_2^{\cdot}$ [64]).

334

335 A beewolf egg of approximately 5 mg emits 0.25 µmol $NO^{\cdot}$ within a period of about 2.5 h, or
336 20.000 µmol/kg*h, a value that is about four orders of magnitude higher than reported baseline
337 levels of $NO^{\cdot}$ synthesis in humans (0.15 - ~4.5 µmol/kg*h [65]), rats (0.6-9 µmol/kg*h [66]) and
338 plants (*Arabidopsis thaliana,* 0.36-3 µmol/kg*h [67]), and even considerably higher than in

bioRxiv preprint doi: https://doi.org/10.1101/495085; this version posted December 24, 2018. The copyright holder for this preprint (which was not certified by peer review) is the author/funder, who has granted bioRxiv a license to display the preprint in perpetuity. It is made available under a CC-BY 4.0 International license.

lipopolysaccharide (LPS)-activated macrophages (~800 µmol/kg*h, estimated from [66]). Despite this extremely high rate of $NO^{\cdot}$ production in beewolf eggs, the amino acid sequence of the beewolf NOS (*Pt-NOS*) is similar to the closely related bees (Fig. S6), indicating that there was little evolutionary change with regard to the gene itself. Moreover, the structure of the *Pt-NOS* gene is largely homologous to other insects, e.g. *Anopheles stephensi* mosquitoes [68].

However, in contrast to adult beewolves, the NOS-mRNA in beewolf eggs lacks exon 14 (Fig. S5). Such alternative splicing that results in different NOS-mRNAs, including the deletion of exons (but others than in beewolves), has been documented in *A. stephensi* in response to *Plasmodium* infection [69]. Moreover, NOS splice variants may result in organ-specific enzymes in other organisms [29]. Presumably, beewolf eggs produce smaller amounts of another NOS splice variant to support signaling functions in the developing embryo.

In adult beewolves, the exon missing in the NOS-mRNA of eggs is located between the binding domains for calmodulin and FMN. Since calmodulin is believed to be responsible for NOS regulation [70] the deletion of an adjacent part might affect the control of NOS activity in beewolf eggs. Thus, the alternative splicing might enable the production of such large amounts of $NO^{\cdot}$. Notably, compared to the cNOS (comprising eNOS, and nNOS) the inducible NOS isoform of vertebrates (iNOS) that generates higher concentrations of $NO^{\cdot}$ to combat microbes lacks a section of about 40 amino acids (120 bp) near the FMN domain. Interestingly, this section is thought to be responsible for autoinhibition of the cNOS [71] and its lack enhances $NO^{\cdot}$ production by the iNOS. The conspicuous similarity between vertebrate iNOS and the NOS in beewolf eggs with regard to the length of the missing section and its position might suggest a convergent modification to achieve a NOS with high synthetic capacity. Whereas vertebrates have evolved another gene, beewolf eggs appear to accomplish a similar effect by alternative splicing of the mRNA.

364

365 The lack of an exon that might circumvent regulation of the NOS and the pattern of *Pt-NOS*
366 expression in the eggs suggest that in beewolf eggs the activity of the enzyme is regulated by gene
367 expression like the NOS in *Plasmodium* infested *A. stephensi* [68] and the iNOS of vertebrates
368 [72,73]. However, in contrast to these cases, in beewolf eggs expression of the Pt-NOS seems not
369 to be induced by immunostimulants but to occur obligatorily at a certain stage in the development
370 of the beewolf embryo.

371

372 Even the combined effect of prey embalming and brood cell fumigation does not provide perfect
373 protection as fungus infestation still causes larval mortality in 5% of the brood cells in the field
374 [16]. Some fungal spores might survive under the bees because they were screened against the
375 gas. Another possibility, namely that strains of the ubiquitous mold fungi that are the main causes
376 of molding in beewolf brood cells [15], have evolved resistance against the toxic effects of
377 $NO^{\cdot}/NO_2^{\cdot}$ seems rather unlikely. There are examples for detoxification of lower concentrations of
378 $NO^{\cdot}$ (mainly by scavengers like flavohemoglobins) in different fungi, including species of *Aspergillus*
379 [75,76]. However, the $NO^{\cdot}/NO_2^{\cdot}$ levels emitted by beewolf eggs are very high and likely affect
380 several very basic biochemical processes, thus making the evolution of an effective resistance
381 unlikely. Moreover, beewolf brood cells are certainly a rare habitat for the ubiquitous mold fungi
382 so that there will be only weak selection for resistance at all.

383

384 While brood cell fumigation clearly retards molding of larval provisions, the antimicrobial effect of
385 $NO^{\cdot}$ and $NO_2^{\cdot}$ might harm the symbiotic *Streptomyces* bacteria that beewolf females apply to the
386 brood cell prior to egg laying [7,46]. Since the symbiotic bacteria are important for the survival of
387 larvae in the cocoon and are vertically transmitted from beewolf mothers to their daughters [47],
388 a considerable number of symbionts have to survive the brood cell fumigation. Possibly, the

389 symbiotic bacteria are resistant to $NO^{\cdot}/NO_2^{\cdot}$. However, that the bacteria are applied to the ceiling
390 of the brood cell might be an adaptation that reduces possible negative effects of the nitrogen
391 oxides since these are heavier than air and will accumulate in the lower part of the brood cell.
392 Additionally, the bacteria are embedded in copious amounts of a secretion consisting of mostly
393 unsaturated hydrocarbons [77] that might shield the bacteria from the fumigants. Moreover,
394 antioxidants in the hydrocarbon matrix could detoxify $NO^{\cdot}$ and $NO_2^{\cdot}$ and protect the symbiotic
395 *Streptomyces* bacteria.
396
397 How could brood cell fumigation with high concentrations of $NO^{\cdot}/NO_2^{\cdot}$ have evolved? Generally, it
398 has been assumed that the primary purpose of $NO^{\cdot}$ was signaling at low concentrations and that
399 the antimicrobial functions of higher concentrations are derived [78]. Assuming a similar scenario
400 for beewolves, small amounts of $NO^{\cdot}$ that were originally produced for developmental processes
401 [23] might have accidentally been released into the confines of the subterranean brood cell and
402 slightly affected the germination or growth of fungi by interfering with regulatory processes
403 [29,79]. Given the severe threat posed by microbes, such initial benefits would have caused strong
404 selection for elevated $NO^{\cdot}$ emission by the eggs. This would have considerably increased progeny
405 survival and might have allowed ancestral beewolves to nest in an expanded range of habitat
406 types, including nesting sites with high risk of microbial infestation, or to exploit highly susceptible
407 but readily available prey species. Brood cell fumigation with large doses of $NO^{\cdot}$ thus represents a
408 key evolutionary innovation. Since $NO^{\cdot}$ is used as an antimicrobial in the immune systems of many
409 animals [80], its deployment as an antifungal gas can be viewed as an innate, externalized immune
410 defense of beewolf eggs. Such externalized components of the immune system have recently been
411 recognized as important and possibly widespread antimicrobial measures [38].
412

413 The clear benefit of brood cell fumigation, however, is probably accompanied by substantial costs
414 in terms of energy and biochemical resources [31]. NO· is synthesized from L-arginine, an amino
415 acid that is an important constituent of many proteins and biochemical pathways [81] and it is an
416 essential amino acid for most insects [82.83] (e.g. phytophagous insects [84], mosquitos [85],
417 aphids [86,87], butterflies [88, 89], true bugs [90], parasitoid wasps [91,92], bees [93,94]). Thus,
418 beewolves have either evolved the capacity to synthesize L-arginine or female beewolves have to
419 provide each egg with sufficient L-arginine for both brood cell fumigation and embryogenesis.
420 Moreover, NO· synthesis by NOS requires the cofactors flavin adenine dinucleotide (FAD), FMN,
421 (6R-)5,6,7,8-tetrahydrobiopterin (BH4) and NADPH [95], thus competing with other metabolic
422 pathways in the developing beewolf embryo.
423
424 One of the most remarkable aspects of our study is that the embryos inside the egg survive the
425 high concentrations of toxic nitrogen oxides during synthesis and emission as well as after its
426 release to the brood cell. This is all the more surprising since beewolf larvae that were accidentally
427 exposed to the gas emitted by eggs died (Strohm, unpublished observations). The synthesis and
428 emission of such high amounts of NO· likely requires a number of concomitant adaptations that
429 protect beewolf embryos against the cytotoxic effects of high concentrations of nitrogen radicals.
430 One possibility is the employment of carrier molecules to transfer NO· to the egg shell. In blood
431 sucking hemipterans, for example, nitrophorins carry NO· to its release site to dilate blood vessels
432 [96]. The mechanistic basis of NO· tolerance of beewolf eggs is of particular interest, since
433 excessive production of NO· due to inflammatory processes [97] or certain diseases (e.g.
434 Alzheimer's disease, [51,52,98,99]) might cause severe pathological complications in humans.
435 Thus, understanding how beewolf eggs avoid the toxic effects of NO· might inspire the
436 development of novel medical applications.
437

bioRxiv preprint doi: https://doi.org/10.1101/495085; this version posted December 24, 2018. The copyright holder for this preprint (which was not certified by peer review) is the author/funder, who has granted bioRxiv a license to display the preprint in perpetuity. It is made available under a CC-BY 4.0 International license.

Our findings reveal a surprising adaptation in a mass-provisioning digger wasp to cope with the threat of pathogen infestation in the vulnerable egg and larval stages. Sanitizing the brood cell environment by producing high amounts of $NO^{\cdot}$ significantly enhances the survival of immatures by reducing fungal growth on their provisions. Given that mass-provisioning and development underground are widespread ecological features among digger wasps and bees and considering the difficulties of detecting volatiles in subterranean nests, such gaseous defenses might be more widespread and as yet underappreciated. In addition to revealing new perspectives on antimicrobial strategies in nature and amplifying the biological significance of $NO^{\cdot}$, beewolves offer unique opportunities to elucidate general questions on the evolution and regulation of NOS as well as the production of and resistance to high concentrations of $NO^{\cdot}$.

Methods

Animals

Beewolf females, *Philanthus triangulum* F. (Apoidea, Crabronidae), were either caught in the field from populations in Franconia (Germany) or were the F1 progeny of such females kept in the laboratory. They were housed in observation cages [21] that provided access to newly completed brood cells. The cages were placed in a room with temperature control (20-22° at night, 25-28°C in the daytime) and were lit for 14 h per day by neon lamps. Honeybees, *Apis mellifera* L. (Apoidea, Apidae), the females' prey, were caught from hive entrances or from flowers and provided *ad libitum*. Honey was provided *ad libitum* in the flight cage for the nutrition of both honeybees and beewolf females.

To obtain freshly laid eggs, observation cages were checked hourly. Completed brood cells were opened, their length and width was measured using calipers and the egg and/or honeybees were removed and used for the experiments. Brood cell volume was estimated as a prolate spheroid with brood cell length as the major and width as the minor axis. The bees in brood cells had been paralyzed, embalmed with lipids [18], and provisioned by beewolf females. Egg volume was estimated to be 4.1±0.5 mm^3 (N = 16) by calculating the volume of a cylinder with the respective length and width of an egg (both determined using a stereomicroscope with eyepiece micrometer).

General experimental procedures

For all experiments beewolf eggs were harvested from brood cells of various females. Eggs were randomly allocated to different treatment groups. Sample sizes refer to independent biological replicates, i.e. each replicate represents a different egg or brood cell – with the exception of

bioRxiv preprint doi: https://doi.org/10.1101/495085; this version posted December 24, 2018. The copyright holder for this preprint (which was not certified by peer review) is the author/funder, who has granted bioRxiv a license to display the preprint in perpetuity. It is made available under a CC-BY 4.0 International license.

quantitative PCR, where several eggs were pooled for one sample (see below). As it is very demanding to obtain beewolf eggs, the availability of eggs of a certain developmental stage was limited. Generally, we used as many eggs as feasible (e.g. for quantitative PCR). For some experiments we decided on a meaningful sample size based on experience from preliminary experiments (e.g. we already knew that inhibition assays with beewolf eggs in Petri dishes were really clear-cut and required only few replicates). Moreover, due to the limited availability of beewolf eggs on a given day, replicates were conducted consecutively over several days.

Fungus inhibition assays

To test whether the time course of fungus growth on bees differed between those carrying an egg and those without egg, we used brood cells (N = 22) that had been provisioned with two bees. We placed each bee individually into an artificial brood cell of natural shape and volume in sand-filled Petri dishes (diameter 10 cm) and with moisture levels similar to natural conditions. Petri dishes were placed in a climate chamber at 25°C in the dark. Bees were carefully checked visually every 24 h for fungus growth without opening the Petri dishes. First signs of fungus infestation (hyphae) were recorded. The experiment was terminated after eleven days since all larvae had finished feeding and spun a cocoon by then. Since these are time event data, we used survival analysis (Kaplan Meier, Breslowe test, SPSS Statistics 21) to compare the timing of fungus infestation of the bees with and without an egg. Larvae hatched on the third day after oviposition and started to feed on the bee. There was no evidence that hatched larvae were able to prevent fungus growth on the bee they occupied or others in the brood cell. However, to take a possible effect of the larva on the experimental bee into account, we carried out the analysis not only over the whole period from oviposition until the larvae spun into a cocoon (11 days) but also for the period from oviposition to the hatching of larvae (3 days). A significant difference already until the third day indicates that this effect was associated with the egg.

bioRxiv preprint doi: https://doi.org/10.1101/495085; this version posted December 24, 2018. The copyright holder for this preprint (which was not certified by peer review) is the author/funder, who has granted bioRxiv a license to display the preprint in perpetuity. It is made available under a CC-BY 4.0 International license.

498

499 We examined whether beewolf eggs emit a volatile antimicrobial by conducting two experiments.
500 For the first test, we used brood cells (N = 16) that contained three bees. The bees were
501 transferred to artificial brood cells in sand-filled Petri dishes as described above. The bee with the
502 egg and one of the bees without egg (the experimental bee) were placed together in the same
503 artificial brood cell but without physical contact. The other bee without egg (the control) was kept
504 alone in another artificial brood cell (in another Petri dish). We monitored the timing of fungus
505 infestation, as described above. We used survival analysis as described above. Again, to take an
506 (unlikely) effect of the larva into account, we also carried out the analysis for the period from
507 oviposition until the larvae hatched (day 3 after oviposition). A significant difference already until
508 day three could only be caused by volatiles emanating from the egg.

509

510 For the second assay, we exposed conidiospores of a diverse spectrum of fungi to the volatiles
511 emanating from beewolf eggs. Petri dishes (10 cm) containing culture medium (malt extract agar
512 or Sabouraud-agar [100]) were inoculated with conidia from different fungal strains (*Aspergillus*
513 *flavus* strain A*,* Trichocomaceae**,** that was isolated from infested beewolf brood cells, [15], N = 20;
514 *A. flavus* strain B*, Mucor circinelloides,* Mucoraceae*; Penicillium roquefortii,* Trichocomaceae;
515 *Candida albicans,* Saccharomycetaceae*; Trichophyton rubrum*, Arthrodermataceae; N = 8 for all
516 the latter strains and species; these were kindly provided by the Department of Hygiene and
517 Microbiology of the Würzburg University Hospital). Conidiospores were harvested by sampling
518 mature fungus colonies that were reared from stock cultures. A suspension of the conidia in sterile
519 water was evenly distributed on the Petri dishes to obtain uniform growth of fungi. To recreate
520 the concentrations of potential antibiotic volatiles in the brood cell, we used small plastic caps (3
521 ml, about the size of a brood cell) to confine test areas on the agar. Freshly laid eggs were placed
522 singly on the bottom of a cap where they readily attached due to their natural stickiness. Each cap

was then placed on a freshly inoculated Petri dish so that the agar under the cap was not in contact with the egg but was exposed to volatiles that emanated from the egg. An empty cap was placed on the same Petri dish as a control. The Petri dishes were incubated in a dark climate chamber at 25°C. Fungus growth under the experimental and control caps was recorded after 24, 48 and 72 h. After 72 h the caps with the hatched larvae were removed, and fungal growth was further recorded after another 24, 48 and 72 h. Since there was either no fungal growth or substantial growth (Fig. 3), the experimental and control areas were compared using binomial tests (software PAST [101]). The qualitative results for all other observation times were identical to those after 24 h.

Identification of the antimicrobial volatile

We hypothesized that nitric oxide ($NO^{\cdot}$) and its main reaction product with oxygen, nitrogen dioxide ($NO_2^{\cdot}$), were the most likely compounds emanating from beewolf eggs. The standard test for the detection of $NO^{\cdot}$ and $NO_2^{\cdot}$ employs the Griess reaction. We used a solution of sulfanilic acid and N-(1-naphthyl)-ethylenediamine (Spectroquant Nitrite Test, Merck, Germany, according to the manufacturer's instructions). The Griess reagent specifically reacts with the nitrite anion (NO_2^-) to form a distinctive red azo dye [102]. $NO^{\cdot}$ reacts with water to form nitrous acid (HNO_2) and can thus be directly verified by the Griess reaction. $NO_2^{\cdot}$, however, disproportionates in water into nitrous acid and nitric acid (HNO_3) and the latter must be reduced to nitrous acid to react with the Griess reagent. Freshly laid beewolf eggs (collected within 2 h after oviposition, N = 11) were placed in the lid of a 1.5 ml reaction tube where they readily attached due to their natural stickiness. Tubes without eggs (N = 11) were used as controls. Then 1 mL of the Griess test solution was added to the tube. For another sample (N = 15) the nitrate, which might be present in the solution, was reduced to nitrite by placing a glass fiber filter disc with small amounts of zinc powder [103] on the surface of the solution. The same setting without an egg was used as control

bioRxiv preprint doi: https://doi.org/10.1101/495085; this version posted December 24, 2018. The copyright holder for this preprint (which was not certified by peer review) is the author/funder, who has granted bioRxiv a license to display the preprint in perpetuity. It is made available under a CC-BY 4.0 International license.

548 (N = 15). The tubes were incubated at 25°C for 24 h, and the occurrence of the red coloration was
549 examined both visually and with a photometer (at 520 nm, Nanophotometer, Implen, Germany).
550 The samples with and without nitrate reduction showed the same results.
551
552 $NO^{\cdot}$ can also be detected by specific fluorescent probes. In particular, diaminorhodamin-4M AM
553 (DAR4M-AM), a cell permeable, photostable fluorescent dye, has a high sensitivity and specificity
554 for $NO^{\cdot}$ [104]). A DAR4M-AM (Alexis Biochemicals, USA) solution was prepared according to the
555 supplier's instructions (10µmol/l in 0.1mol/l phosphate buffer, pH 7.4). To verify and to visualize
556 the emission of $NO^{\cdot}$ from the egg, paralyzed honeybees either with freshly laid eggs (N = 8) or
557 controls without eggs (N = 8) were sprayed with the DAR4M-AM solution using a nebulizer (the
558 egg itself was screened from droplets during spraying) and kept in the dark (at 25°C in artificial
559 brood cells as described above). After 20 h, the bees were examined under a fluorescence
560 microscope (Axiophot II, Zeiss, Germany, filter set 43: excitation 520-570 nm, emission 535-675
561 nm) and digital photos were taken (Nikon DS-2 Mv, Nikon Japan) at constant exposure times, to
562 allow comparison of fluorescence intensity. Due to the size of the bees, several pictures had to be
563 taken in the X,Y plane as well as along the Z axis. Pictures along the z-axis were stacked using the
564 software Combine-ZP (www.hadleyweb.pwp.blueyonder.co.uk). Then these stacks were stitched
565 using Photoshop Elements 5 (PSE5, Adobe Systems Inc. USA). Since small peripheral background
566 parts within the frame of the stacked and stitched picture were "empty" these parts were filled
567 with other background parts by using the clone stamp tool. Images were corrected for contrast
568 and sharpness using PSE5 with identical settings for experimental and control specimens.
569
570 DAR4M-AM can also be used to detect $NO^{\cdot}$ in tissues. Aliquots of 0.1-0.5 µl of the DAR4M-AM
571 solution (see above) were injected into beewolf eggs (within 1 h after oviposition, N = 64, in N = 45
572 eggs the embryo survived and developed) with a custom made microinjector equipped with glass

bioRxiv preprint doi: https://doi.org/10.1101/495085; this version posted December 24, 2018. The copyright holder for this preprint (which was not certified by peer review) is the author/funder, who has granted bioRxiv a license to display the preprint in perpetuity. It is made available under a CC-BY 4.0 International license.

capillaries (Eppendorf Femtotips II, Eppendorf, Germany) under microscopic control. The eggs were kept in dark chambers (as above), and fluorescence was observed directly after injection and 1, 3, 5, 24, 48 and 72 h later. Control eggs injected with buffer only (N = 10) were monitored in the same way to assess autofluorescence. For comparison, eggs of two other Hymenoptera (*Osmia bicornis*, Apoidea, Megachilidae, N = 12, and *Ampulex compressa*, Apoidea, Ampulicidae, N = 9; eggs from both species were obtained from our own laboratory populations) as well as freshly hatched beewolf larvae (N = 4) were injected with the DAR4M-AM solution and monitored in the same way. Fluorescence was examined under a fluorescence microscope and documented with a digital camera as described above. Contrast and sharpness of the images were optimized using Photoshop Elements 5 (Adobe, USA) with identical settings for all specimens.

Quantification, time course and temperature dependence of $NO^{\cdot}$ production

Iodometry provides a simple but sensitive, reliable and precise method to quantify strong oxidants. To assess the amount of emitted nitrogen oxides, we placed freshly laid eggs (N = 233) individually into the lid of 1.5 ml reaction tubes where they readily attached due to their natural stickiness. Then 1 ml of a potassium iodide-starch solution (containing 1% KI and 1% soluble starch in distilled water) was added, the reaction tube was closed and kept for 24 h at 28°C in a dark climate chamber. Oxidation of iodide results in iodine that forms a blue complex with starch [103]. The degree of coloration was quantified by measuring the absorbance at 590 nm in a spectrophotometer (Uvikon 860, Kontron, Germany). To assess the absolute amount of the oxidant, the solutions were subsequently calibrated by titration with a reference solution of sodium thiosulfate (concentration: 0.001 M; Merck, Germany) until the blue color of the iodine-starch complex disappeared.

bioRxiv preprint doi: https://doi.org/10.1101/495085; this version posted December 24, 2018. The copyright holder for this preprint (which was not certified by peer review) is the author/funder, who has granted bioRxiv a license to display the preprint in perpetuity. It is made available under a CC-BY 4.0 International license.

To establish the time course of gas production, individual beewolf eggs (N = 4) were transferred within 1 h after oviposition into the lid of reaction tubes and kept in a dark climate chamber at 28°C. Every hour, the cap with the egg was transferred to another reaction tube with fresh iodide-starch solution. Immediately after removal of the egg from a reaction tube, absorbance of the solution was measured at 590 nm as described above.

To investigate the temperature dependence of gas production, tubes with a newly laid egg and iodide-starch solution (as described above, N = 33 in total) were placed in a rack (with white background) inside a climate chamber and incubated at seven different constant temperatures (20, 22.5, 24, 25.5, 27, 28.5 and 30°C). The time course of coloration of the iodide-starch solution was recorded using a digital camera (Canon EOS 20D, Canon, Japan) programmed to take pictures at 30 min intervals. The onset of gas production could be easily determined since the color of the solution turned from clear to dark blue from one picture to the next, i.e. within a 30 min interval. A quadratic regression curve was fitted to the data (SPSS Statistics 21) and the Q_{10} value for the temperature dependence was estimated.

Detection of NOS activity in egg tissue

To detect NOS activity in the egg tissue, we used fixation-insensitive NADPH diaphorase staining with nitroblue tetrazolium [105,106]. Eggs were fixed in PBS containing 4% paraformaldehyde for 2 h at 4°C, followed by cryoprotection in PBS with 12% sucrose for 20 h. The tissue was soaked in Tissue Tec (Sakura Finetek, Netherlands) for 30 min, frozen, and 10 µm sections were cut on a cryostat microtome (CM3000, Leica, Germany). The sections were incubated for 60 min at 30°C with 50 mmol/l Tris-HCl, pH 7.8, 0.1% Triton X-100, and 0.2 mmol/l nitroblue tetrazolium chloride in the presence or absence (each N = 5) of 0.2 mmol/l β-NADPH to demonstrate fixation-insensitive NADPH diaphorase activity. The sections were dehydrated, mounted with Depex

bioRxiv preprint doi: https://doi.org/10.1101/495085; this version posted December 24, 2018. The copyright holder for this preprint (which was not certified by peer review) is the author/funder, who has granted bioRxiv a license to display the preprint in perpetuity. It is made available under a CC-BY 4.0 International license.

(Serva, Germany) and observed under a compound microscope (Zeiss Axiophot II). Photos were taken with a digital camera (Nikon DS-2 Mv). To cover the whole egg, two pictures had to be stitched (Photoshop Elements 5, Adobe USA) and contrast and sharpness were optimized.

Phenology of NOS gene expression

If NOS is responsible for $NO^{\cdot}$ production in beewolf eggs, the time pattern of *NOS* gene expression should largely resemble the time course of $NO^{\cdot}$ production by showing a pronounced peak several hours after egg laying (the timing of the peak depending on temperature). We used reverse transcription and real time quantitative PCR to quantify the NOS mRNA in beewolf eggs at different times after oviposition. Since the amount of mRNA that could be obtained from single eggs was insufficient to get reproducible results, we pooled 10 eggs in one trial and 24 eggs in a second trial for each of four different time intervals after oviposition (4-5, 9-10, 14-15 and 19-20 h after oviposition, all kept at 25°C) as well as the respective number of freshly hatched larvae. The eggs and larvae were removed from the brood cells at the specified times, shock frozen with liquid nitrogen and stored at -80°C. The RNA of each sample was extracted using the peqGOLD total RNA Kit (Peqlab, Germany) according to the supplier's instructions and eluted with 20 µL RNase free water. An aliquot of 3 µL of the RNA was digested with DNaseI (Fermentas, Lithuania) and transcribed into cDNA with BioScript (Bioline, Germany) using an Oligo-dT primer (Fermentas, Lithuania) in a final volume of 20 µL. As a reference for basic levels of gene expression during the experimental period, mRNA of the housekeeping gene β-actin was quantified and the ratio of NOS/β-actin mRNA was calculated for each sample.

For quantitative PCR, we established new primers for both the NOS and β-actin genes of *P. triangulum* (based on the complete *NOS* sequences, see below) (NOS_qPCR_F1 & R4; Actin_qPCR_F1 & R1, Table S1). All primers were intron-overlapping to avoid the measurement of

bioRxiv preprint doi: https://doi.org/10.1101/495085; this version posted December 24, 2018. The copyright holder for this preprint (which was not certified by peer review) is the author/funder, who has granted bioRxiv a license to display the preprint in perpetuity. It is made available under a CC-BY 4.0 International license.

647 contaminating genomic DNA. The NOS and actin primers amplified fragments of 312bp and 321bp,
648 respectively. The qPCRs were performed on an Eppendorf Realplex cycler (Eppendorf, Germany)
649 in a final volume of 25 µL, containing 1 µL of template cDNA (1 µL of the 20 µL RT reaction mix),
650 2.5 µL of each primer (10 pmol/l) and 12.5 µL of SYBR Green Mix (SensiMixPlus SYBR Mit,
651 Quantace, UK). Standard curves were established by using 10^{-9} – 10^{-3} ng of PCR products as
652 template. A NanoDrop TM1000 spectrophotometer (Peqlab, Germany) was used to measure DNA
653 concentrations of the templates for the standard curves. PCR conditions were as follows: 95°C for
654 5 min, followed by 50 cycles of 56°C (β-actin) or 65°C (NOS) for 60 s, 72°C for 60 s and 95°C for 60
655 s. Then a melting curve analysis was performed by increasing the temperature from 60°C to 95°C
656 within 20 min. Based on the standard curves, the amount of NOS and β-actin template and their
657 ratio was calculated.
658
659 NOS inhibition assay
660 To verify the role of NOS in $NO^{\cdot}$ production by beewolf eggs, we used an inhibition assay [107].
661 Since L-arginine is the substrate for $NO^{\cdot}$ production by NOS, we injected either an inhibiting L-
662 arginine analogue or, for controls, a non-inhibiting enantiomer into freshly laid beewolf eggs.
663 Chemicals were dissolved in 0.1 mol/l phosphate buffer pH 7.4. Using a microinjector (see above)
664 eggs were injected with about 0.2 µl of 1.5 mol/l solutions of (1) the competitive inhibitor Nω-
665 nitro-L-arginine methylester (L-NAME, Sigma-Aldrich, USA) (experimental group, N = 14), or (2) the
666 non-inhibiting Nω-nitro-D-arginine methylester (D-NAME, Sigma-Aldrich, USA) (control group 1, N
667 = 9) or (3) not injected at all (N = 14, control group 2). Each egg of the three groups was placed
668 individually in the lid of a reaction tube with an iodide-starch solution as described above and
669 incubated for 24 h at 28°C. Then $NO^{\cdot}$ production was assessed by measuring absorbance of the
670 solution with a photometer (Implen Nanophotometer) at 590 nm. Statistical comparison of the

671 groups was conducted using Mann-Whitney U-tests with correction after Holm [108] (SPSS
672 Statistics 18).
673
674 Sequencing of the *P. triangulum* nitric oxide synthase gene (*Pt-NOS*) and mRNA
675 DNA was extracted from female beewolf heads with the Epicentre MasterPure Complete DNA and
676 RNA Purification kit (Epicentre, USA) according to the manufacturer's guidelines for tissue
677 extraction. Eggs for RNA extraction were kept at a temperature of 27.5°C (range 26-29°C),
678 collected 14-15 h after oviposition, immediately frozen in liquid nitrogen and stored at -70°C until
679 RNA extraction. Twenty eggs were pooled for extraction and homogenized by repeatedly pipetting
680 in lysis buffer of the PeqGOLD Total RNA kit (Peqlab, Germany). Samples were processed according
681 to the kit manual and frozen at -70°C. For the full transcriptome sequencing (to obtain the 5'
682 terminal region) RNA was extracted from the antennae of eight frozen female beewolves
683 according to manufacturer's protocol 1 of the innuPrep RNA Mini Kit (Analytik Jena, Germany).
684
685 Most of the beewolf *NOS* gene was amplified and sequenced by primer walking. Sequencing
686 reactions were performed by a commercial service (Seqlab, Germany). Four degenerate primers
687 (NOS860fwd2, NOS1571rev1, NOS_seq_F1_deg, and NOS_seq_R1_deg) were designed (Table S1)
688 based on published *NOS* sequences of *Drosophila melanogaster* (U25117.1), *Apis mellifera*
689 (AB204558.1), *Anopheles stephensi* (AH007775.1), *Rhodnius prolixus* (U59389.1), *Manduca sexta*
690 (AF062749.1) and *Nasonia vitripennis* (NM_001168232.1). First, the central region (~700bp,
691 between NOS860fwd2 & NOS1571rev1) was amplified and sequenced. Based on this sequence, we
692 designed a pair of *P. triangulum* specific primers (NOS_qPCR_F2 and NOS_qPCR_R2, Table S1).
693 Using one specific central and one degenerate terminal primer (NOS_seq_F1_deg and
694 NOS_seq_R1_deg, Table S1), respectively, fragments of 4-5 kb were amplified and sequenced by
695 primer walking, which yielded the central 9.5 kb of the *NOS* gene.

696

697 Fragments larger than 2 kb were amplified with the PeqGOLD Mid-Range PCR System on a
698 thermocycler (TGradient, Biometra, Germany). Reaction volumes of 12.5 µL contained 1 µL DNA
699 template, 50 mmol/l Tris-HCl (pH 9.1), 14 mmol/l $(NH_4)_2SO_4$, 1.75 mmol/l $MgCl_2$, 350 mmol/l of
700 each dNTP, 400 mmol/l of each primer and 0.5 U 'MidRange PCR' enzyme mix. An initial 3 min
701 melting step at 94°C was followed by 35 cycles of 0.5 min at 94°C, 0.5 min at 58°C and 3 min+20
702 sec per cycle at 68°C and a final extension time of 20 min at 68°C.

703

704 Fragments up to 2 kb were amplified using the PeqGOLD Taq. Reaction volumes of 12.5 µL
705 contained 1 µL of DNA template, 50 mmol/l Tris-HCl pH 9.1, 14 mmol/l $(NH_4)_2SO_4$, 3 mmol/l $MgCl_2$,
706 240 µmol of each dNTP, 800 nmol/l of each primer and 0.5 U Taq. An initial 3 min melting step at
707 95°C was followed by 35 cycles of 1 min at 95°C, 1 min at 60°C and 2 min at 72°C and a final
708 extension time of 3 min at 72°C.

709

710 The 3' terminus was sequenced following the 3' RACE protocol [109]. Briefly, cDNA was generated
711 by reverse transcription with a poly-T primer. Before reverse transcription, co-extracted DNA was
712 digested using DNaseI (New England Biolabs, UK).The DNA digestion mix contained 1 mmol/l Tris-
713 HCl, 0.25 mmol/l $MgCl_2$ and 1 mmol/l $CaCl_2$ and 0.4 U DNaseI. DNA was digested for 10 min at
714 37°C, followed by DNase inactivation for 10 min at 75°C. The final reverse transcription mix
715 contained 25 mmol/l KCL, 10 mmol/l Tris-HCl, 0,6 mmol/l $MgCl_2$, 2 mmol/l DTT, 4 µmol poly-T or
716 gene specific primer, 0.5 mmol/l of each dNTP and 200 U of BioSkript Moloney Murine Leukaemia
717 Virus reverse transcriptase (Bioline, Germany). The entire digestion mixture was incubated with
718 the primer for 5 min at 70°C to enable primer annealing, then cooled on ice. Reverse transcription
719 was carried out for 1 h at 42°C and the enzyme was subsequently inactivated for 10 min at 70°C.
720 The cDNA including the 3' terminal region was amplified with the specific primer NOS_seq_3-F3

721 and a 'poly-T adapter primer', i.e. a polyT primer to which a specific adapter sequence was added
722 [109] (Table S1). Subsequently, a nested PCR was performed using a second specific primer
723 (NOS_seq_3-F6) and a primer that contained only the specific adapter sequence of the 'polyT
724 adapter primer' to increase PCR specificity (Table S1, same PCR conditions as above).
725
726 The 5' terminal region of 200 bp was obtained from a full transcriptome sequencing approach of
727 female antennae, which covered the full-length NOS mRNA sequence. RNA sequencing was
728 performed by a commercial service provider (Fasteris, Switzerland), using the HiSeq TM2000
729 Sequencing System (Illumina, USA) with 100 bp single reads, on 5 µg total RNA isolated from
730 female *P. triangulum* antennae. CLC Genomics Workbench was used for sequence assembly of the
731 resulting 75 million reads. Reads were quality-trimmed with standard settings and subsequently
732 assembled using the following CLC parameters: nucleotide mismatch cost = 2; insertion cost = 2;
733 deletion cost = 2; length fraction = 0.3; similarity = 0.9. Conflicts among the individual bases were
734 resolved by voting for the base with highest frequency. Contigs shorter than 250 bp were
735 discarded.
736
737 To sequence the entire NOS transcript from eggs, cDNA was generated by reverse transcription
738 with a poly-T primer and additionally a specific, central NOS_RT_R1 primer, followed by PCR
739 amplification using various primer combinations to cover the whole transcript sequence (Table
740 S1). Additionally, the sequence of the 5' terminal region was confirmed by RT-PCR of mRNA from
741 *P. triangulum* eggs, using primers NOS_seq_5-F6 and NOS_seq_5-R3 (Table S1) and subsequent
742 sequencing.
743
744 Even though we used a large number of primers to cover the gene, we did not find sections with
745 signals for two different bases at the same site. Thus we infer that there is only one *NOS* gene in

746 the *P. triangulum* genome, as in most invertebrates [110]. In addition, the transcriptome dataset
747 did not reveal any other transcript that was annotated as nitric oxide synthase.
748
749 The GenBank accession numbers for the *P. triangulum NOS* (*Pt-NOS*) gene sequence is: KJ425525,
750 for the NOS mRNA of *P. triangulum* eggs: KJ425526, and for the NOS mRNA in *P. triangulum*
751 female antennae: KJ425527.
752
753 Phylogenetic analysis of *NOS* gene sequences
754 NOS coding sequences of 23 insect species from five orders were acquired from the NCBI
755 database. Along with the *P. triangulum NOS* sequence, these were translated and aligned using
756 Geneious (Version 6.0.5, created by Biomatters, Geneious, New Zealand). The highly variable 5'
757 end was trimmed. An approximately-maximum-likelihood tree was created with FastTree [111,
758 112]. Local support values were estimated with the Shimodaira-Hasegawa test based on 1,000
759 samples without re-optimizing the branch lengths for the resampled alignments [111]. Bayesian
760 estimates were made with the program MrBayes 3.1.2 [113-115). The MCMC analysis was
761 conducted under a mixed amino acid rate model (prset aamodelpr= mixed). After 1,000,000
762 generations, with trees sampled every 1000 generations, the standard deviation of split
763 frequencies was consistently lower than 0.01. We discarded the first 100 of the sampled trees
764 (10% burn-in) and computed a 50% majority rule consensus tree with posterior probability values
765 for every node. The trees estimated by both methods were nearly identical, so they were
766 combined into a single figure.
767
768

Acknowledgements: We are grateful to Wilhelm Boland for advice, to Nathalie Moske for technical assistance, to Stephan Schneuwly for providing the microinjection device and, in particular, to Jon Seger and Jeremy Field for valuable comments on earlier drafts of the manuscript.

Author Contributions

Conceptualization ES

Methodology ES TE MK GH JR

Formal Analysis ES TE

Investigation ES TE GH JR MK

Resources ES JR

Writing – Original Draft Preparation ES TE

Writing – Review & Editing ES TE GH MK JR

Visualization ES TE

Supervision ES

Funding Acquisition ES

Statement on competing interests: We declare that none of the authors has any competing interests.

793 References

794 1. Gilliam M, Taber III S, Richardson GV. Hygienic behavior of honey bees in relation to
795 chalkbrood disease. Apidologie. 1983;14(1):29-39.
796 2. Herzner G, Schlecht A, Dollhofer V, Parzefall C, Harrar K, Kreuzer A, et al. Larvae of the
797 parasitoid wasp Ampulex compressa sanitize their host, the American cockroach, with a blend
798 of antimicrobials. Proc Natl Acad Sci U S A. 2013;110(4):1369-74.
799 3. Vilcinskas A, Mukherjee K, Vogel H. Expansion of the antimicrobial peptide repertoire in the
800 invasive ladybird Harmonia axyridis. Proc R Soc Lond **B** Biol Sci. 2013;280(1750).
801 4. Gross J, Schumacher K, Schmidtberg H, Vilcinskas A. Protected by fumigants: beetle perfumes
802 in antimicrobial defense. J Chem Ecol. 2008;34(2):179-88.
803 5. Hooper LV, Littman DR, Macpherson AJ. Interactions between the microbiota and the immune
804 system. Science. 2012;336(6086):1268-73.
805 6. Iwasaki A, Medzhitov R. Regulation of adaptive immunity by the innate immune system.
806 Science. 2010;327(5963):291-5.
807 7. Kaltenpoth M, Göttler W, Herzner G, Strohm E. Symbiotic Bacteria Protect Wasp Larvae from
808 Fungal Infestation. Curr Biol. 2005;15(5):475-9.
809 8. Flórez LV, Scherlach K, Gaube P, Ross C, Sitte E, Hermes C, et al. Antibiotic-producing
810 symbionts dynamically transition between plant pathogenicity and insect-defensive
811 mutualism. Nat Commun. 2017;8.
812 9. Janzen D. Why fruits rot, seeds mold, and meat spoils. Am Nat. 1977;111:691-713.
813 10. Rozen D, Engelmoer D, Smiseth P. Antimicrobial strategies in burying beetles breeding on
814 carrion. Proc Natl Acad Sci U S A. 2008;105(46):17890-5.
815 11. Wilson K, Cotter SC. Host-parasite interactions and the evolution of immune defense. Adv
816 Study Behav. 2013;45:81-174.

bioRxiv preprint doi: https://doi.org/10.1101/495085; this version posted December 24, 2018. The copyright holder for this preprint (which was not certified by peer review) is the author/funder, who has granted bioRxiv a license to display the preprint in perpetuity. It is made available under a CC-BY 4.0 International license.

12. Tranter C, Graystock P, Shaw C, Lopes J, Hughes W. Sanitizing the fortress: protection of ant brood and nest material by worker antibiotics. Behav Ecol Sociobiol. 2014;68(3):499-507.
13. Arce AN, Smiseth PT, Rozen DE. Antimicrobial secretions and social immunity in larval burying beetles, Nicrophorus vespilloides. Anim Behav. 2013;86(4):741-5.
14. Strohm E, Linsenmair KE. Allocation of parental investment among individual offspring in the European beewolf *Philanthus triangulum* F. (Hymenoptera: Sphecidae). Biol J Linn Soc Lond. 2000;69:173-92.
15. Engl T, Bodenstein B, Strohm E. Mycobiota in the brood cells of the European beewolf, Philanthus triangulum (Hymenoptera: Crabronidae). Europ J Entomol. 2016;113:271.
16. Strohm E, Linsenmair KE. Females of the European beewolf preserve their honeybee prey against competing fungi. Ecol Entomol. 2001;26(2):198-203.
17. Herzner G, Ruther J, Goller S, Schulz S, Goettler W, Strohm E. Structure, chemical composition and putative function of the postpharyngeal gland of the emerald cockroach wasp, Ampulex compressa (Hymenoptera, Ampulicidae). Zoology. 2011;114:36-45.
18. Herzner G, Schmitt T, Peschke K, Hilpert A, Strohm E. Food wrapping with the postpharyngeal gland secretion by females of the European beewolf Philanthus triangulum. J chem ecol. 2007;33(4):849-59.
19. Herzner G, Strohm E. Fighting fungi with physics: Food wrapping by a solitary wasp prevents water condensation. Curr Biol. 2007;17(2):R46-R7.
20. Herzner G, Engl T, Strohm E. Cryptic combat against competing microbes is a costly component of parental care in a digger wasp. Anim Behav. 2011;82(2):321-8.
21. Strohm E, Linsenmair KE. Leaving the cradle: how beewolves (*Philanthus triangulum* F.) obtain the necessary spatial information for emergence. Zoology. 1994/95;98:137-46.
22. Mücke W, Lemmen C. Duft und Geruch: Wirkungen und gesundheitliche Bedeutung von Geruchsstoffen. Landsberg am Lech: ecomed - Storck GmbH; 2010.

23. Andersen D, Colombani J, Leopold P. Coordination of organ growth: principles and outstanding questions from the world of insects. Trends Cell Biol. 2013;23(7):336-44.
24. Soegiarto L, Wills R, Seberry J, Leshem Y. Nitric oxide degradation in oxygen atmospheres and rate of uptake by horticultural produce. Postharvest Biol Technol. 2003;28(2):327-31.
25. Mur LA, Mandon J, Cristescu SM, Harren FJ, Prats E. Methods of nitric oxide detection in plants: a commentary. Plant Science. 2011;181(5):509-19.
26. Fang FC. Perspectives series: host/pathogen interactions. Mechanisms of nitric oxide-related antimicrobial activity. J Clin Invest. 1997;99(12):2818.
27. Lai T, Li B, Qin G, Tian S. Oxidative damage involves in the inhibitory effect of nitric oxide on spore germination of Penicillium expansum. Curr microbiol. 2011;62(1):229-34.
28. Tsikas D. Analysis of nitrite and nitrate in biological fluids by assays based on the Griess reaction: appraisal of the Griess reaction in the L-arginine/nitric oxide area of research. J Chromatogr B. 2007;851(1):51-70.
29. Röszer T. The biology of subcellular nitric oxide. Heidleberg: Springer; 2012.
30. Regulski M, Tully T. Molecular and biochemical characterization of dNOS: a Drosophila Ca2+/calmodulin-dependent nitric oxide synthase. Proc Natl Acad Sci U S A. 1995;92(20):9072-6.
31. Rivero A. Nitric oxide: an antiparasitic molecule of invertebrates. Trends Parasitol. 2006;22(5):219-25.
32. Whitten M, Sun F, Tew I, Schaub G, Soukou C, Nappi A, et al. Differential modulation of< i> Rhodnius prolixus</i> nitric oxide activities following challenge with< i> Trypanosoma rangeli</i>,< i> T. cruzi</i> and bacterial cell wall components. Insect Biochem Mol Biol. 2007;37(5):440-52.
33. Akira S, Uematsu S, Takeuchi O. Pathogen recognition and innate immunity. Cell. [Review]. 2006 Feb;124(4):783-801.

34. Hirano M, Das S, Guo P, Cooper MD. The Evolution of Adaptive Immunity in Vertebrates. In: Alt FW, Austen KF, Honjo T, Melchers F, Uhr JW, Unanue ER, editors. Adv Immunol, Vol 109. San Diego: Elsevier Academic Press Inc; 2011. p. 125-57.

35. Lemaitre B, Hoffmann J. The host defense of Drosophila melanogaster. Annu Rev Immunol. [Review; Book Chapter]. 2007;25:697-743.

36. Siva-Jothy MT, Moret Y, Rolff J. Insect immunity: An evolutionary ecology perspective. In: Simpson SJ, editor. Advances in Insect Physiology, Vol 32. San Diego: Elsevier Academic Press Inc; 2005. p. 1-48.

37. Gorman M, Kankanala P, Kanost M. Bacterial challenge stimulates innate immune responses in extra-embryonic tissues of tobacco hornworm eggs. Insect Mol Biol. 2004;13(1):19-24.

38. Otti O, Tragust S, Feldhaar H. Unifying external and internal immune defences. Trends Ecol Evol. 2014;29(11):625-34.

39. Degenkolb T, Düring R-A, Vilcinskas A. Secondary metabolites released by the burying beetle Nicrophorus vespilloides: chemical analyses and possible ecological functions. J Chem Ecol. 2011;37(7):724-35.

40. Vander Meer RK, Morel L. Ant queens deposit pheromones and antimicrobial agents on eggs. Naturwissenschaften. 1995;82(2):93-5.

41. Marchini D, Marri L, Rosetto M, Manetti AG, Dallai R. Presence of Antibacterial Peptides on the Laid Egg Chorion of the MedflyCeratitis capitata. Biochem Biophys Res Commun. 1997;240(3):657-63.

42. Flórez LV, Biedermann PH, Engl T, Kaltenpoth M. Defensive symbioses of animals with prokaryotic and eukaryotic microorganisms. Nat Prod Rep. 2015;32(7):904-36.

43. Tragust S, Mitteregger B, Barone V, Konrad M, Ugelvig LV, Cremer S. Ants disinfect fungus-exposed brood by oral uptake and spread of their poison. Curr Biol. 2013;23(1):76-82.

44. Gross J, Schmidtberg H. Glands of leaf beetle larvae–protective structures against attacking predators and pathogens. Research on Chrysomelidae, Volume 2: Brill; 2009. p. 177-90.

45. Lopes RB, Laumann RA, Blassioli-Moraes MC, Borges M, Faria M. The fungistatic and fungicidal effects of volatiles from metathoracic glands of soybean-attacking stink bugs (Heteroptera: Pentatomidae) on the entomopathogen Beauveria bassiana. J Invertebr Pathol. 2015;132:77-85.

46. Kroiss J, Kaltenpoth M, Schneider B, Schwinger MG, Hertweck C, Maddula RK, et al. Symbiotic streptomycetes provide antibiotic combination prophylaxis for wasp offspring. Nat Chem Biol. 2010.

47. Kaltenpoth M, Roeser-Mueller K, Koehler S, Peterson A, Nechitaylo TY, Stubblefield JW, et al. Partner choice and fidelity stabilize coevolution in a Cretaceous-age defensive symbiosis. Proc Natl Acad Sci U S A. 2014;111(17):6359-64.

48. Moroz LL, Kohn AB. On the comparative biology of Nitric oxide (NO) synthetic pathways: parallel evolution of NO-mediated signaling. Adv Exp Biol. 2007;1:1-44.

49. Thomas DD, Miranda KM, Citrin D, Espey MG, Wink DA. Nitric oxide. Combat Medicine: Springer; 2003. p. 23-60.

50. Filipovic MR, Koh AC, Arbault Sp, Niketic V, Debus A, Schleicher U, et al. Striking Inflammation from Both Sides: Manganese (II) Pentaazamacrocyclic SOD Mimics Act Also as Nitric Oxide Dismutases: A Single Cell Study. Angew Chem Int Ed Engl. 2010;49(25):4228-32.

51. Lüth H-J, Münch G, Arendt T. Aberrant expression of NOS isoforms in Alzheimerâ€™s disease is structurally related to nitrotyrosine formation. Brain research. 2002;953(1):135-43.

52. Pacher Pl, Beckman JS, Liaudet L. Nitric oxide and peroxynitrite in health and disease. Physiol Rev. 2007;87(1):315-424.

53. Titheradge MA. Nitric oxide in septic shock. Biochimica et Biophysica Acta (BBA)-Bioenergetics. 1999;1411(2):437-55.

bioRxiv preprint doi: https://doi.org/10.1101/495085; this version posted December 24, 2018. The copyright holder for this preprint (which was not certified by peer review) is the author/funder, who has granted bioRxiv a license to display the preprint in perpetuity. It is made available under a CC-BY 4.0 International license.

916 54. Burke AJ, Sullivan FJ, Giles FJ, Glynn SA. The yin and yang of nitric oxide in cancer progression.
917 Carcinogenesis. 2013;34(3):503-12.
918 55. Beckman JS, Koppenol WH. Nitric oxide, superoxide, and peroxynitrite: the good, the bad, and
919 the ugly. Am J Physiol-Cell Physiol. 1996;40(5):C1424.
920 56. Wink DA, Hines HB, Cheng RY, Switzer CH, Flores-Santana W, Vitek MP, et al. Nitric oxide and
921 redox mechanisms in the immune response. J Leukoc Biol. 2011;89(6):873-91.
922 57. Jones ML, Ganopolsky JG, Labbé A, Wahl C, Prakash S. Antimicrobial properties of nitric oxide
923 and its application in antimicrobial formulations and medical devices. Appl Microbiol
924 Biotechnol. 2010;88(2):401-7.
925 58. Feelisch M. The chemical biology of nitric oxide—an outsider's reflections about its role in
926 osteoarthritis. Osteoarthritis and Cartilage. 2008;16:S3-S13.
927 59. Canessa P, Larrondo LF. Environmental responses and the control of iron homeostasis in
928 fungal systems. Appl Microbiol Biotechnol. 2013;97(3):939-55.
929 60. Bogdan C. Nitric oxide and the immune response. Nat Immunol. 2001;2(10):907-16.
930 61. Vaughn MW, Kuo L, Liao JC. Estimation of nitric oxide production and reactionrates in tissue
931 by use of a mathematical model. Am J Physiol Heart Circ Physiol. 1998;274(6):H2163-H76.
932 62. Ghaffari A, Miller C, McMullin B, Ghahary A. Potential application of gaseous nitric oxide as a
933 topical antimicrobial agent. Nitric Oxide. 2006;14(1):21-9.
934 63. Lazar E, Wills R, Ho B, Harris A, Spohr L. Antifungal effect of gaseous nitric oxide on mycelium
935 growth, sporulation and spore germination of the postharvest horticulture pathogens,
936 Aspergillus niger, Monilinia fructicola and Penicillium italicum. Lett Appl Microbiol.
937 2008;46(6):688-92.
938 64. Administration USOSaH. Directorate of Technical Support and Emergency Management
939 (DTSEM). United States Department of Labor; 2014 [cited 2014]; Available from:
940 https://www.osha.gov/dts/.

65. Castillo L, Beaumier L, Ajami AM, Young VR. Whole body nitric oxide synthesis in healthy men determined from [15N] arginine-to-[15N] citrulline labeling. Proc Natl Acad Sci U S A. 1996;93(21):11460-5.

66. Wu G, Flynn NE, Flynn SP, Jolly CA, Davis PK. Dietary protein or arginine deficiency impairs constitutive and inducible nitric oxide synthesis by young rats. J Nutr. 1999;129(7):1347-54.

67. Zeidler D, Zähringer U, Gerber I, Dubery I, Hartung T, Bors W, et al. Innate immunity in Arabidopsis thaliana: lipopolysaccharides activate nitric oxide synthase (NOS) and induce defense genes. Proc Natl Acad Sci U S A. 2004;101(44):15811-6.

68. Luckhart S, Vodovotz Y, Cui L, Rosenberg R. The mosquito Anopheles stephensi limits malaria parasite development with inducible synthesis of nitric oxide. Proc Natl Acad Sci U S A. 1998;95(10):5700-5.

69. Luckhart S, Li K. Transcriptional complexity of the *Anopheles stephensi* nitric oxide synthase gene. Insect Biochem Mol Biol. 2001;31(3):249-56.

70. Smith BC, Underbakke ES, Kulp DW, Schief WR, Marletta MA. Nitric oxide synthase domain interfaces regulate electron transfer and calmodulin activation. Proc Natl Acad Sci U S A. 2013;110(38):E3577-E86.

71. Salerno JC, Harris DE, Irizarry K, Patel B, Morales AJ, Smith SM, et al. An autoinhibitory control element defines calcium-regulated isoforms of nitric oxide synthase. J Biol Chem. 1997;272(47):29769-77.

72. Wong M-L, Rettori V, Amer A-S, Bongiorno PB, Canteros G, McCann SM, et al. Inducible nitric oxide synthase gene expression in the brain during systemic inflammation. Nat Med. 1996;2(5):581-4.

73. Morris Jr SM. Arginine synthesis, metabolism, and transport: regulators of nitric oxide synthesis. Cell Mol Biol Nitric Oxide. 1999:57-85.

74. Gao S-H, Fan L, Yuan Z, Bond PL. The concentration-determined and population-specific antimicrobial effects of free nitrous acid on Pseudomonas aeruginosa PAO1. Appl Microbiol Biotechnol. 2015;99(5):2305-12.

75. de Paulo Martins V, Dinamarco TM, Curti C, Uyemura SA. Classical and alternative components of the mitochondrial respiratory chain in pathogenic fungi as potential therapeutic targets. J Bioenerg Biomembr. 2011;43(1):81-8.

76. Zhou S, Fushinobu S, Nakanishi Y, Kim S-W, Wakagi T, Shoun H. Cloning and characterization of two flavohemoglobins from Aspergillus oryzae. Biochem Biophys Res Commun. 2009;381(1):7-11.

77. Kaltenpoth M, Schmitt T, Strohm E. Hydrocarbons in the antennal gland secretion of female European beewolves, Philanthus triangulum (Hymenoptera, Crabronidae). Chemoecology. 2009;19(4):219-25.

78. Fang FC. Antimicrobial reactive oxygen and nitrogen species: concepts and controversies. Nat Rev Microbiol. 2004;2(10):820-32.

79. Wang J, Higgins VJ. Nitric oxide has a regulatory effect in the germination of conidia of Colletotrichum coccodes. Fungal Genet Biol. 2005;42(4):284-92.

80. Bogdan C, Röllinghoff M, Diefenbach A. Reactive oxygen and reactive nitrogen intermediates in innate and specific immunity. Curr Opin Immunol. 2000;12(1):64-76.

81. Morris Jr SM. Regulation of arginine availability and its impact on NO synthesis. Nitric oxide biol pathobiol. 2000:187-97.

82. Barbehenn RV, Reese JC, Hagen KS. The food of insects. Ecol Entomol. 1999:83-121.

83. Payne SH, Loomis WF. Retention and loss of amino acid biosynthetic pathways based on analysis of whole-genome sequences. Eukaryot cell. 2006;5(2):272-6.

84. Berenbaum MR. Turnabout is fair play: secondary roles for primary compounds. J Chem Ecol. 1995;21(7):925-40.

85. Uchida K. Balanced amino acid composition essential for infusion-induced egg development in the mosquito (Culex pipiens pallens). J Insect Physiol. 1993;39(7):615-21.

86. Sasaki T, Ishikawa H. Production of essential amino acids from glutamate by mycetocyte symbionts of the pea aphid, Acyrthosiphon pisum. J Insect Physiol. 1995;41(1):41-6.

87. Gündüz EA, Douglas A. Symbiotic bacteria enable insect to use a nutritionally inadequate diet. Proc R Soc Lond B Biol Sci. 2009;276(1658):987-91.

88. Erhardt A, Rusterholz H-P. Do peacock butterflies (Inachis io L.) detect and prefer nectar amino acids and other nitrogenous compounds? Oecologia. 1998;117(4):536-42.

89. O'Brien DM, Boggs CL, Fogel ML. Pollen feeding in the butterfly Heliconius charitonia: isotopic evidence for essential amino acid transfer from pollen to eggs. Proc R Soc Lond B Biol Sci. 2003;270(1533):2631-6.

90. Mesquita RD, Vionette-Amaral RJ, Lowenberger C, Rivera-Pomar R, Monteiro FA, Minx P, et al. Genome of Rhodnius prolixus, an insect vector of Chagas disease, reveals unique adaptations to hematophagy and parasite infection. Proc Natl Acad Sci U S A.. 2015;112(48):14936-41.

91. Thompson S. The amino acid requirements for larval development of the hymenopterous parasitoid Exeristes roborator Fabricius (Hymenoptera: Ichneumonidae). Comp Biochem Physiol A Mol Integr Physiol. 1976;53(2):211-3.

92. Barrett M, Schmidt J. A comparison between the amino acid composition of an egg parasitoid wasp and some of its hosts. Entomol Exp Appl. 1991;59(1):29-41.

93. De Groot A. Amino acid requirements for growth of the honeybee (Apis mellifica L.). Experientia. 1952;8(5):192-4.

94. Weiner CN, Hilpert A, Werner M, Linsenmair KE, Blüthgen N. Pollen amino acids and flower specialisation in solitary bees. Apidologie. 2010;41(4):476-87.

95. Förstermann U, Sessa WC. Nitric oxide synthases: regulation and function. Eur Heart J. 2012;33(7):829-37.

96. Davies S-A. Nitric oxide signalling in insects. Insect Biochem Mol Biol. 2000;30(12):1123-38.

97. Guzik T, Korbut R, Adamek-Guzik T. Nitric oxide and superoxide in inflammation. J Physiol Pharmacol. 2003;54:469-87.

98. Calabrese V, Mancuso C, Calvani M, Rizzarelli E, Butterfield DA, Stella AMG. Nitric oxide in the central nervous system: neuroprotection versus neurotoxicity. Nat Rev Neurosci. 2007;8(10):766-75.

99. Pautz A, Art J, Hahn S, Nowag S, Voss C, Kleinert H. Regulation of the expression of inducible nitric oxide synthase. Nitric Oxide. 2010;23(2):75-93.

100. Atlas RM. Handbook of microbiological media: CRC press; 2004.

101. Hammer Ø, Harper D, Ryan P. PAST-Palaeontological statistics. www uv es/~ pardomv/pe/2001_1/past/pastprog/past pdf, acessado em. 2001;25(07):2009.

102. Guevara I, Iwanejko J, Dembinska-Kieca A, Pankiewicz J, Wanat A, Anna P, et al. Determination of nitrite/nitrate in human biological material by the simple Griess reaction. Clin Chim Acta. 1998;274(2):177-88.

103. Jander G, Blasius E. Einführung in das anorganisch-chemische Praktikum. Stuttgart: Hirzel; 1971.

104. Kojima H, Hirotani M, Urano Y, Kikuchi K, Higuchi T, Nagano T. Fluorescent indicators for nitric oxide based on rhodamine chromophore. Tetrahedron Lett. 2000;41(1):69-72.

105. Virgili M, Poli A, Beraudi A, Giuliani A, Villani L. Regional distribution of nitric oxide synthase and NADPH-diaphorase activities in the central nervous system of teleosts. Brain Res. 2001;901(1):202-7.

106. Müller U. Ca2+/Calmodulinâ€dependent Nitric Oxide Synthase in Apis mellifera and Drosophila melanogaster. Eur J Neurosci. 1994;6(8):1362-70.

107. Willmot M, Gibson C, Gray L, Murphy S, Bath P. Nitric oxide synthase inhibitors in experimental ischemic stroke and their effects on infarct size and cerebral blood flow: a systematic review. Free Radic Biol Med. 2005;39(3):412-25.

108. Holm S. A simple sequentially rejective multiple test procedure. Scand Stat Theory Appl. 1979:65-70.

109. Sambrook J, Russell DW. Molecular cloning: a laboratory manual. Volume 1–3. Cold Spring Harbor, New York: Cold Spring Harbor Laboratory Press; 2001.

110. Labbe P, McTaggart SJ, Little TJ. An ancient immunity gene duplication in< i> Daphnia magna</i>: RNA expression and sequence analysis of two nitric oxide synthase genes. Dev Comp Immunol. 2009;33(9):1000-10.

111. Price MN, Dehal PS, Arkin AP. FastTree 2 - approximately maximum-likelihood trees for large alignments. PLoS One. 2010;5(3):e9490.

112. Price MN, Dehal PS, Arkin AP. FastTree: computing large minimum evolution trees with profiles instead of a distance matrix. Mol Biol Evol. 2009;26(7):1641-50.

113. Huelsenbeck JP, Ronquist F. MRBAYES: Bayesian inference of phylogenetic trees. Bioinformatics. 2001;17(8):754-5.

114. Huelsenbeck JP, Ronquist F, Nielsen R, Bollback JP. Bayesian inference of phylogeny and its impact on evolutionary biology. Science. 2001;294(5550):2310-4.

115. Ronquist F, Huelsenbeck JP. MrBayes 3: Bayesian phylogenetic inference under mixed models. Bioinformatics. 2003;19(12):1572-4.

bioRxiv preprint doi: https://doi.org/10.1101/495085; this version posted December 24, 2018. The copyright holder for this preprint (which was not certified by peer review) is the author/funder, who has granted bioRxiv a license to display the preprint in perpetuity. It is made available under a CC-BY 4.0 International license.

Supporting information

SI Figures

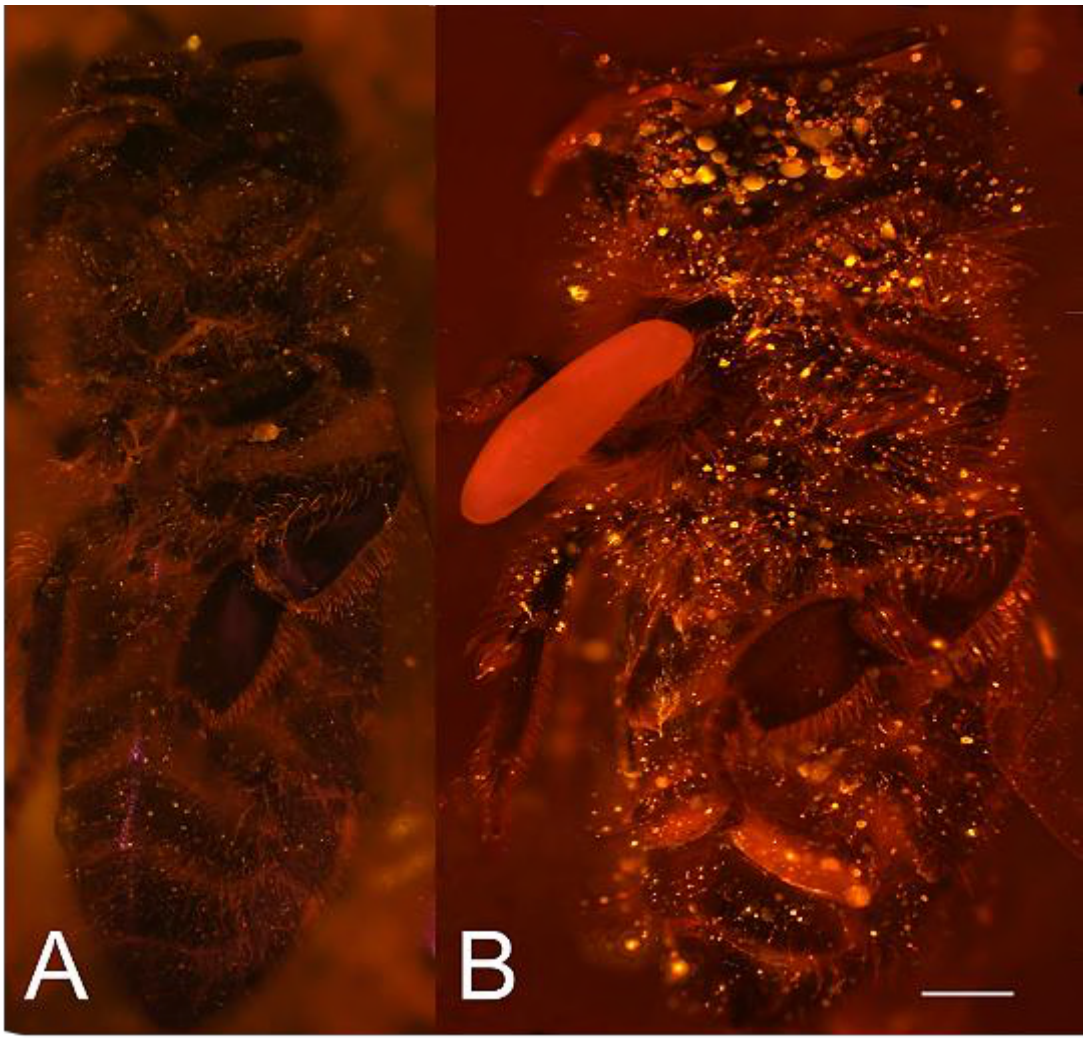

Figure S1. Visualization of $NO^{\cdot}$ emission by beewolf eggs using fluorescence imaging. (A) Honeybee from a brood cell without an egg and (B) honeybee with egg. Both bees were sprayed with a solution of the $NO^{\cdot}$ specific fluorescence probe DAR4M-AM. Only the droplets on the bee with the egg (B) show a bright yellow and orange fluorescence indicating the presence of $NO^{\cdot}$. Image is a composite of multiple pictures of the x/y plane and z-axis. Scale bar = 1 mm.

bioRxiv preprint doi: https://doi.org/10.1101/495085; this version posted December 24, 2018. The copyright holder for this preprint (which was not certified by peer review) is the author/funder, who has granted bioRxiv a license to display the preprint in perpetuity. It is made available under a CC-BY 4.0 International license.

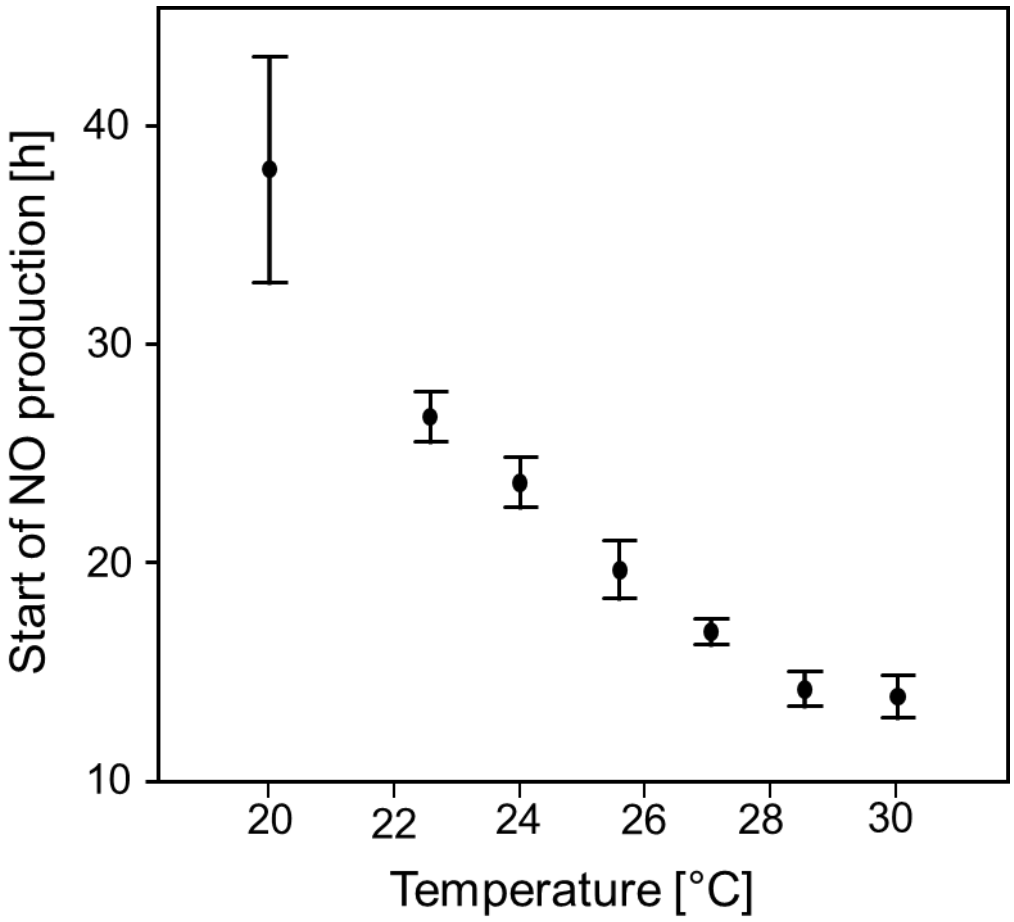

Figure S2. Start of $NO^{\cdot}$ emission (h after oviposition) as a function of temperature. Beewolf eggs were kept at different temperatures and the onset of $NO^{\cdot}$ release was assessed using the color change of an iodide starch solution as monitored by a digital camera at 30min intervals. Symbols are means ± SD (Quadratic regression: $R^2 = 0.98$, N = 33, $p < 0.001$; $Q_{10} = 2.74$). Source data file: Fig S2 Source data - start of NO emission.xlsx

bioRxiv preprint doi: https://doi.org/10.1101/495085; this version posted December 24, 2018. The copyright holder for this preprint (which was not certified by peer review) is the author/funder, who has granted bioRxiv a license to display the preprint in perpetuity. It is made available under a CC-BY 4.0 International license.

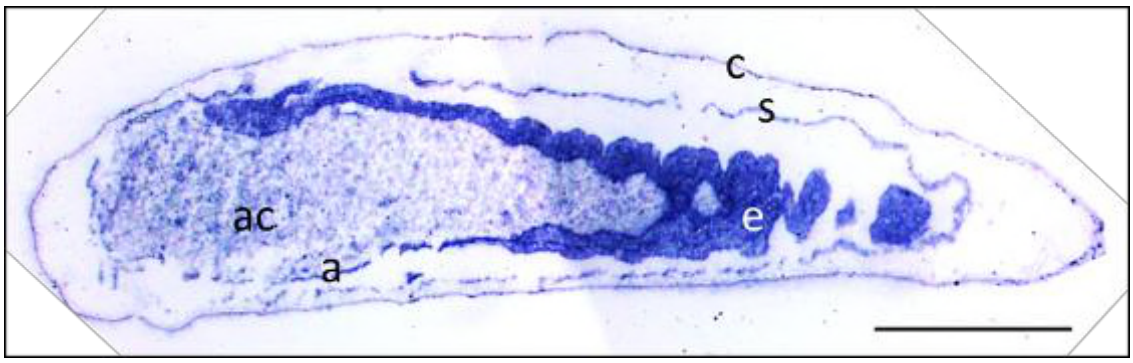

Figure S3. Photomicrograph of a longitudinal section of a beewolf egg showing fixation insensitive NADPH-diaphorase activity. Strong blue staining in the embryonic tissue indicates the presence of reduced nitroblue tetrazolium demonstrating NOS activity (c=cuticle, s=serosa, e= embryo, a=amnion, ac= amnion cavity, scale bar = 1 mm, image composed from two separate photos of the left and right parts of the egg.).

bioRxiv preprint doi: https://doi.org/10.1101/495085; this version posted December 24, 2018. The copyright holder for this preprint (which was not certified by peer review) is the author/funder, who has granted bioRxiv a license to display the preprint in perpetuity. It is made available under a CC-BY 4.0 International license.

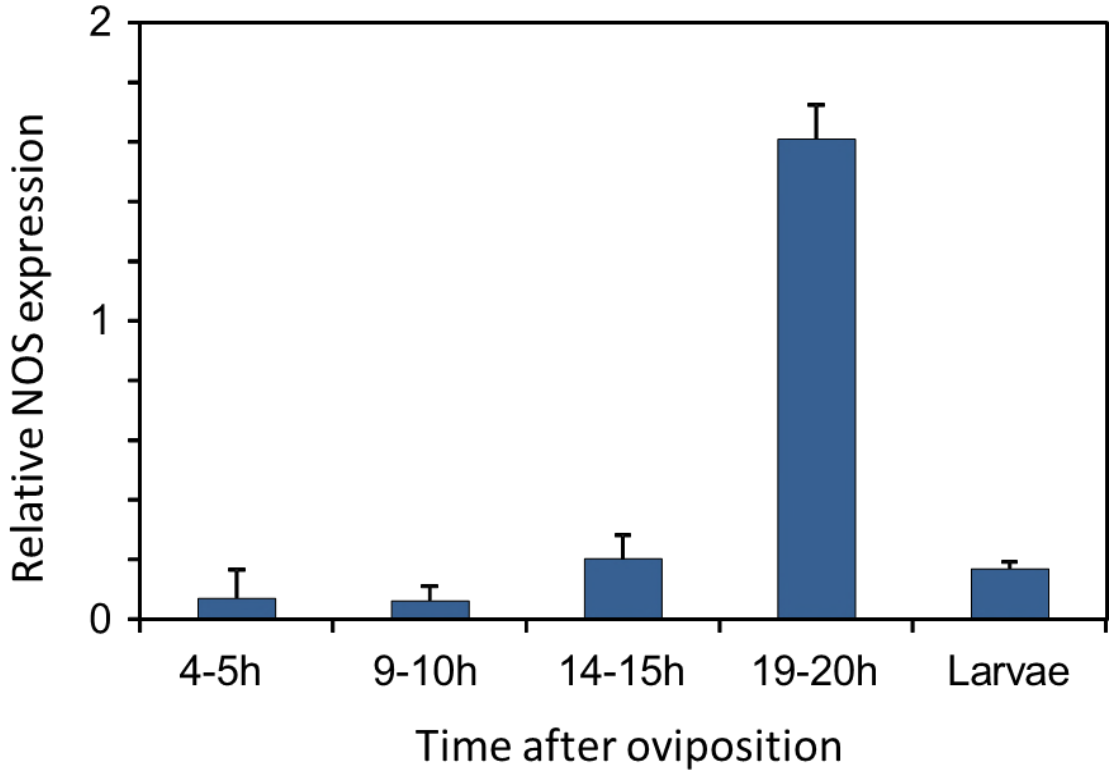

Figure S4. Gene expression of NOS relative to ß-actin in beewolf eggs at different times after oviposition and in freshly hatched larvae. Two trials were conducted, one with 19 and one with 24 eggs per time point. Mean ratios of NOS-mRNA to ß-Actin-mRNA are shown (with standard deviations), as determined by Q-RT-PCR. Source data file: Fig S4 Source data - NOS gene expression.xlsx

bioRxiv preprint doi: https://doi.org/10.1101/495085; this version posted December 24, 2018. The copyright holder for this preprint (which was not certified by peer review) is the author/funder, who has granted bioRxiv a license to display the preprint in perpetuity. It is made available under a CC-BY 4.0 International license.

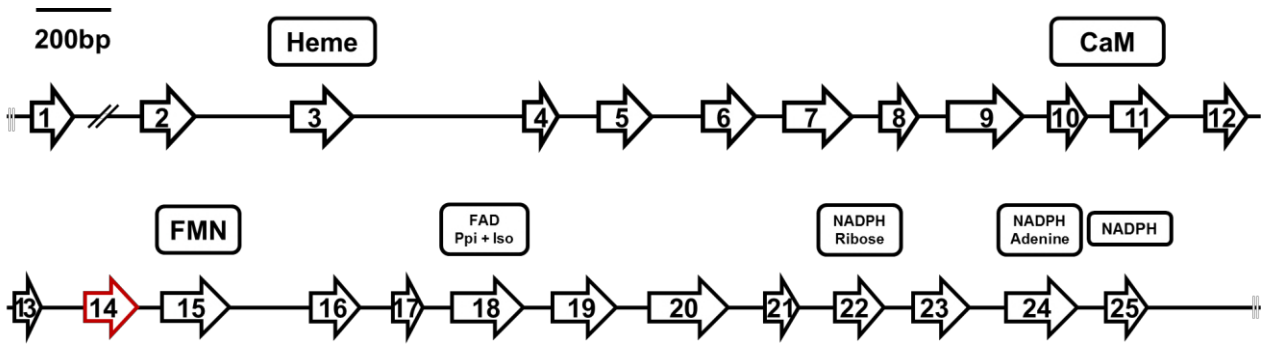

Figure S5. Structure of the *Pt-NOS* gene indicating position and length of exons. Exon 14 (red) is missing in the NOS mRNA in beewolf eggs compared to adults. Presumed cofactor-binding domains as deduced from homologous sequences of the *NOS* of *Anopheles stephensi* [68, 69] are indicated for heme, calmodulin (CaM), FMN, FAD pyrophosphate (FAD PPi) and FAD isoalloxazine (FAD Iso), NADPH ribose, NADPH adenine, and NADPH.

bioRxiv preprint doi: https://doi.org/10.1101/495085; this version posted December 24, 2018. The copyright holder for this preprint (which was not certified by peer review) is the author/funder, who has granted bioRxiv a license to display the preprint in perpetuity. It is made available under a CC-BY 4.0 International license.

36

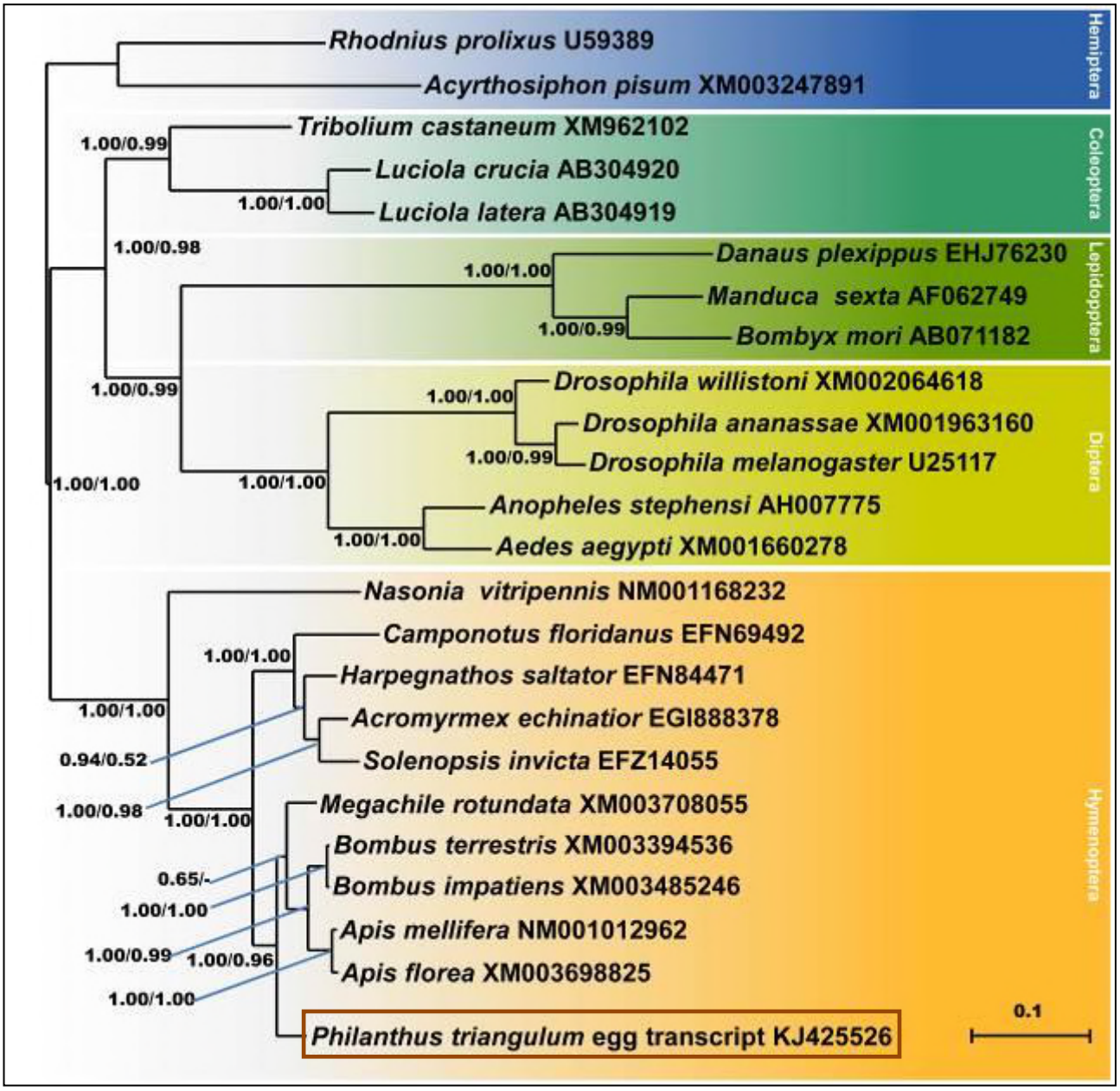

37

38 Figure S6. Consensus tree obtained from Bayesian analysis of NOS amino acid sequences from five orders of
39 insects (distinguished by different colors), including the NOS sequences of *P. triangulum* eggs (lowermost
40 entry). Values at the nodes represent Bayesian posterior probabilities and local support values (FastTree
41 analysis), respectively. Scale bar represents 0.1 changes per site.

42

43